

# **An investigation for the appearance of long range nuclear potential on the ultra low energy nuclear synthesis**

S. Oryu, T. Watanabe, Y. Hiratsuka, and M. Takeda

Faculty of Science and Technology, Tokyo University of Science,  
2641 Yamazaki, Noda, Chiba 278 8510, Japan

September 6, 2019, EFB24 @ Surrey UK.

**Supported by MHI Innovation Accelerator LLC**

# Motivation & Starting Point

Phys. Rev. C86 , 044001 (2012),  
Few—Body Syst.59, 51 (2018).

The author proposed a Long Range (**GPT**) Potential which appears, not only **at the 3-body Break-up Threshold (3BT)**, but also **at the Quasi 2-body Threshold (Q2T)**.

The GPT Potential represents

- 1) a **Yukawa-type** potential for shorter range,
- 2) but a  **$1=r^n$  -type** potential for longer range.

# Energy dependent quasi 2 - body AGS - Born

(E2Q)

$$Z_{\alpha\beta}(q, q'; E) = \frac{g_{\alpha}(p)g_{\beta}(p')(1 - \delta_{\alpha\beta})}{(E + \varepsilon_B) - q^2/2\mu} \rightarrow \infty$$

at (Q2T):  $p = p' = 0$ ,  $E_{cm} = (E + \varepsilon_B) = 0$ ,  $q = 0$

For  $E_{cm} < 0$ : with  $\sigma^2 = 2\mu |E_{cm}|$ ,  $0 < C_{\alpha\beta}$

$$Z_{\alpha\beta} \rightarrow \frac{g_{\alpha}(0)g_{\beta}(0)(1 - \delta_{\alpha\beta})}{-|E_{cm}| - q^2/2\mu} = -\frac{C_{\alpha\beta}}{q^2 + \sigma^2}$$

Therefore, the **Fourier transformation** becomes

$$F \left[ Z_{\alpha\beta}(q, q'; E) \right] = V_0 \frac{e^{-\sigma r}}{r} : \quad V_0 < 0$$

To avoid the divergence at Q2T ,

Adopt a **statistical average** with a weight :  $P$

$$P = \frac{\sigma^{2\gamma+1} e^{-a\sigma}}{\rho}$$

$$\rho = \int_0^{\infty} \sigma^{2\gamma+1} e^{-a\sigma} d\sigma = \frac{\Gamma(2\gamma + 2)}{a^{2\gamma+2}}$$

$$\begin{aligned} L \{U^{(0)}(\Delta, \sigma; r)\} &\equiv V_0 \frac{1}{\rho} \int_0^{\infty} \sigma^{2\gamma+1} e^{-a\sigma} \frac{e^{-\sigma r/2}}{r} d\sigma \\ &= V_0 \frac{a^{2\gamma+2}}{r(r/2 + a)^{2\gamma+2}} \end{aligned}$$

GPT-potential: below the Q2T, or 3BT ( $E_{cm} < 0$ ) with parameters  $a$  and  $\gamma$ , where  $V_0 (< 0)$  is a potential depth.

$$V_0 \frac{a^{2\gamma+2}}{r(r/2 + a)^{2\gamma+2}}$$

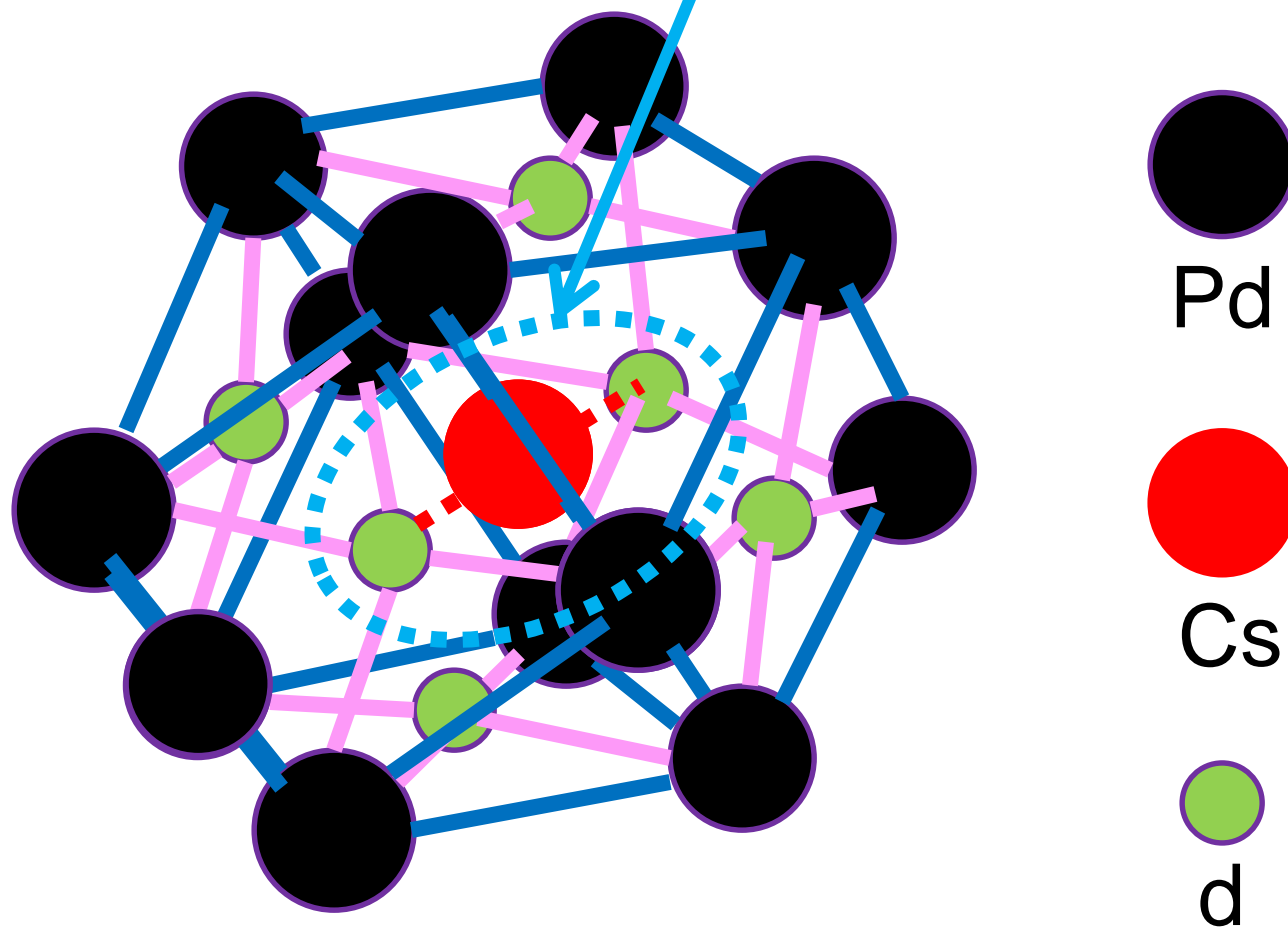
$\gamma$	$r \ll a$	GPT-potential	$a \ll r$
-1	$V_0/r$	$V_0/r$	$V_0/r$
-1/2	$V_0 e^{-r/2a} / r$	$V_0(2a) / [r(r + 2a)]$	$V_0(2a) / r^2$
0	$V_0 e^{-2r/2a} / r$	$V_0(2a)^2 / [r(r + 2a)^2]$	$V_0(2a)^2 / r^3$
1/2	$V_0 e^{-3r/2a} / r$	$V_0(2a)^3 / [r(r + 2a)^3]$	$V_0(2a)^3 / r^4$
1	$V_0 e^{-4r/2a} / r$	$V_0(2a)^4 / [r(r + 2a)^4]$	$V_0(2a)^4 / r^5$
3/2	$V_0 e^{-5r/2a} / r$	$V_0(2a)^5 / [r(r + 2a)^5]$	$V_0(2a)^5 / r^6$
2	$V_0 e^{-6r/2a} / r$	$V_0(2a)^6 / [r(r + 2a)^6]$	$V_0(2a)^6 / r^7$

The **GPT**-potential includes automatically the **Efimov-like potential in any systems**.

In order **to confirm the GPT** potential, we **investigate** ultra low energy reactions  
 $^{135}\text{Cs}(2d,\gamma)^{139}\text{La}$ ;  $^{137}\text{Cs}(2d,\gamma)^{141}\text{La}$

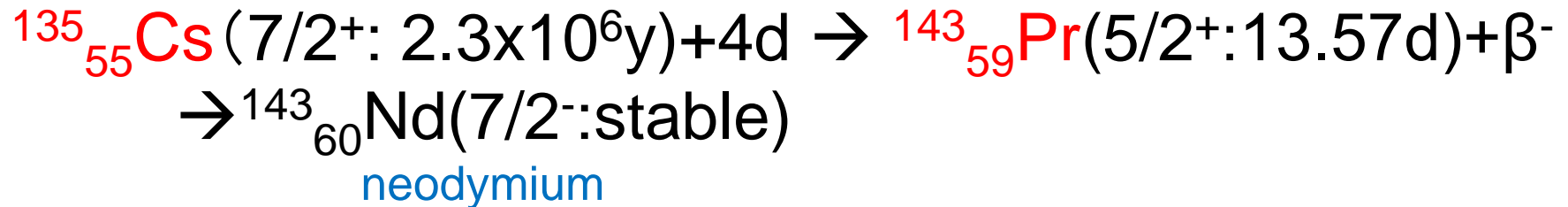
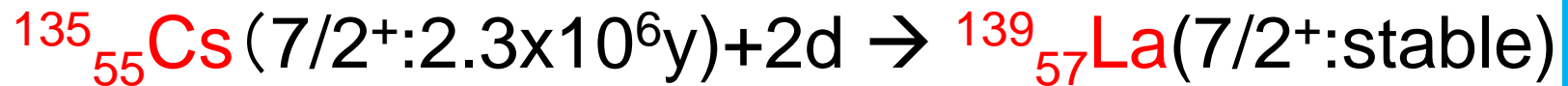
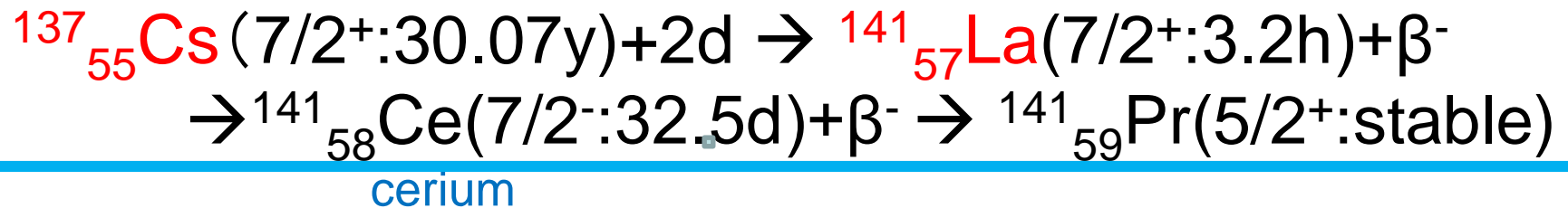
**by** the three-ion quasi-molecule  $\text{CsD}_2$   
in the Pd-cluster with a form:  $\text{CsD}_2\text{Pd}_{12}$ .

Define **quasi molecules**  $\text{CsD}_2$ ,  $\text{CsD}_4$  and  $\text{CsD}_6$



$\text{Cs-d}_6\text{-Pd}_{12}$   
Cub-octahedron

Our calculation:



Calculate **D-Cs-D** (d-Cs-d) three-body bound states and **wave functions**.



# Cs-D<sub>6</sub>-Pd<sub>12</sub> Cub-octahedron

Number of surface:

8-regular triangles + 6-regular squares  
=14 surfaces

24-sides

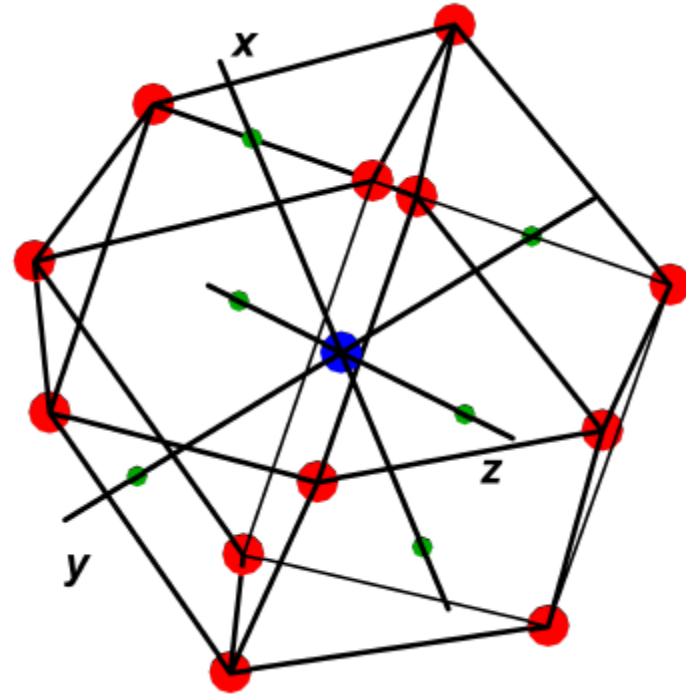
12-apexes

Surface area  $S = (6 + 2\sqrt{3})a^2$

Volume  $V = \frac{5\sqrt{2}}{3}a^3$

Radius of  $a$   
the circumscribed sphere

Pd ● Cs ● D ●

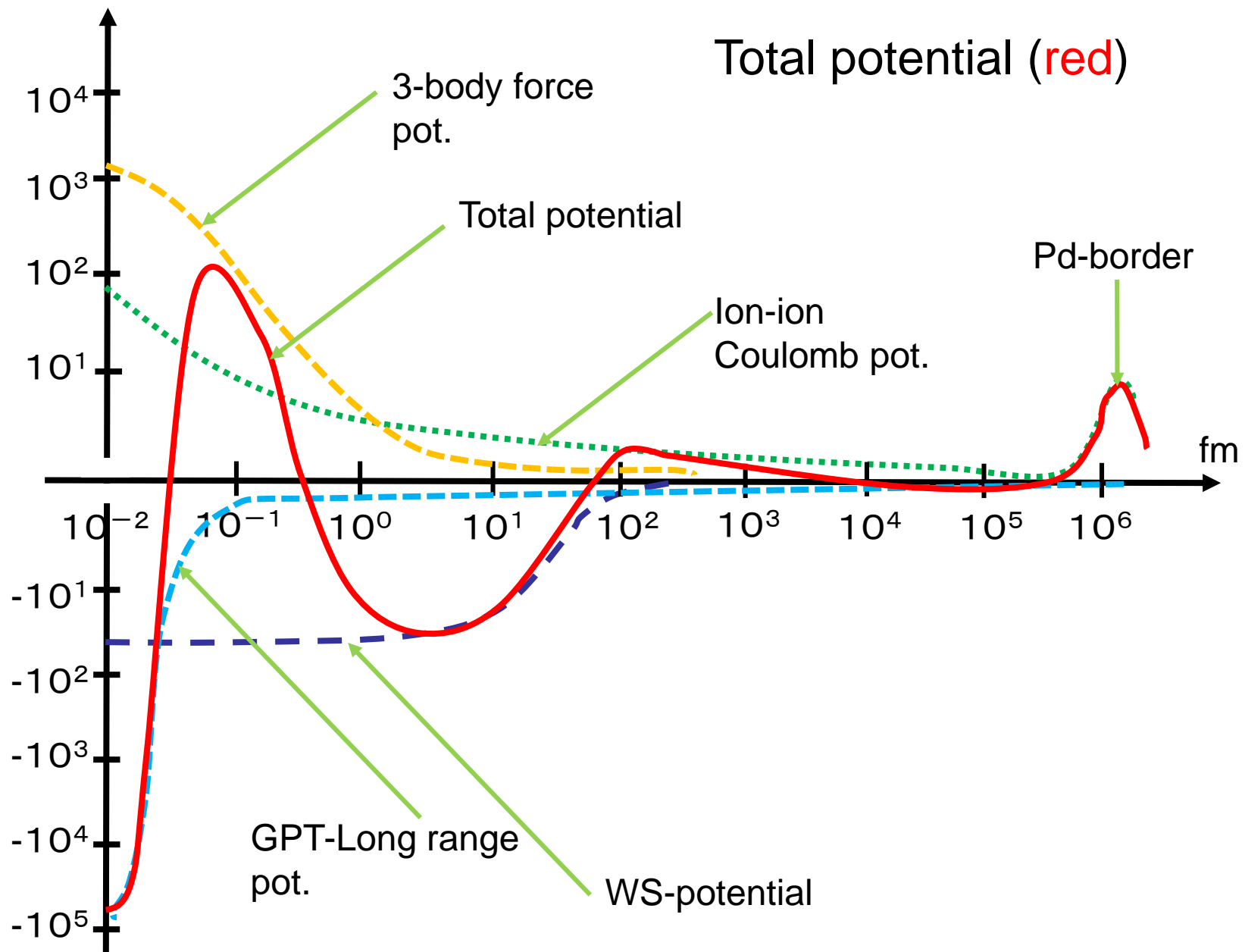


D exists inside of the surface

Pd - Pd distance  $R_{Pd} = a = 5.2 \text{ au} \approx 2.75172144 \times 10^5 \text{ fm}$

D - Cs distance  $R_D = 3.1 \text{ au} \approx 1.64044932 \times 10^5 \text{ fm}$

$1 \text{ au} = 0.591772 \text{ \AA}$



# Potentials in the three-body system

1) Nuclear potential:

$$V_W^{N_i N_j}(r_{ij}) = \frac{V_{W0}^{N_i N_j}}{1 + \exp\left(\frac{r_{ij} - R_W^{N_i N_j}}{a_W^{N_i N_j}}\right)} : \quad \boxed{WS - potential}$$

$$V_{W0}^{Cs d} = -79.30 \text{ MeV}, \quad V_{W0}^{dd} = -27.57 \text{ MeV}, \quad R_W^{Cs d} = 10.21 \text{ fm},$$

$$R_W^{dd} = 1.49 \text{ fm}, \quad a_W^{Cs d} = 0.4 \text{ fm}, \quad a_W^{dd} = 0.3 \text{ fm},$$

2) Coulomb potential:

$$V_c^{N_i N_j}(r_{ij}) = \begin{cases} \frac{Z_i Z_j e^2}{8\pi R} \left[ 3 - \left( \frac{r_{ij}}{R_c^{N_i N_j}} \right)^2 \right] & \text{for } r \leq R \\ \frac{Z_i Z_j e^2}{8\pi r_{ij}} & \text{for } R \leq r \end{cases}$$

$$R_c^{CsH} = 10.21 \text{ fm}, \quad R_c^{H_1 H_2} = 10.21 \text{ fm}.$$

3) Pd-N<sub>i</sub> potential: one-body potential

$$V_c^{\text{PdN}_i}(r_i) = V_{c0}^{\text{Pd}} \left( \frac{r_i}{a_c^{\text{Pd}}} \right)^{10} \exp \left\{ - \left( \frac{r_i - a_c^{\text{Pd}}}{b_c^{\text{Pd}}} \right)^2 \right\}$$

$$V_{c0}^{\text{Pd}} = 1.0 \times 10^{-4} \text{ MeV}, \quad a_{c0}^{\text{Pd}} = 5.0 \times 10^5 \text{ fm},$$

$$b_{c0}^{\text{Pd}} = 3.1623 \times 10^5 \text{ fm}.$$

Pd position  $1.57 \times 10^6$  fm, 2.73 MeV height.

4) Three-cluster potential:

$$V_t(r_1, r_2, r_3) = V_{t0} \exp \left[ - \left( \frac{r_{12}}{a_t} \right)^2 - \left( \frac{r_{23}}{a_t} \right)^2 - \left( \frac{r_{31}}{a_t} \right)^2 \right]$$

$$V_{t0} = 1800 \text{ MeV}, \quad a_t = 3.0 \text{ fm}.$$

## 5) Long range potential:

$$V_e(r_1, r_2, r_3) = \frac{V_{e0}}{\left(\frac{r_{12}}{a_e}\right)^l + \left(\frac{r_{23}}{a_e}\right)^m + \left(\frac{r_{31}}{a_e}\right)^n + 1}$$

Our 3-body Long Range Potential

take  $l = m = n = 2$  (*Efimov case*).

$$V_e(r_1, r_2, r_3) = \frac{V_{e0}}{\left(\frac{r_{12}}{a_e}\right)^2 + \left(\frac{r_{23}}{a_e}\right)^2 + \left(\frac{r_{31}}{a_e}\right)^2 + 1} = \frac{V_{e0} a_e^2}{r_{12}^2 + r_{23}^2 + r_{31}^2 + a_e^2}$$

$$V_{e0} = -80000 \text{ MeV}, \quad a_e = 500 \text{ fm.}$$



$$V_e(r_1, r_2, r_3) = \frac{V_{e0} a_e^2}{r_{12}^2 + r_{23}^2 + r_{31}^2 + a_e^2}$$

Lorentz-type

$$V_{e0} = -80000 \text{ MeV}, \quad a_e = 5000 \text{ fm.}$$



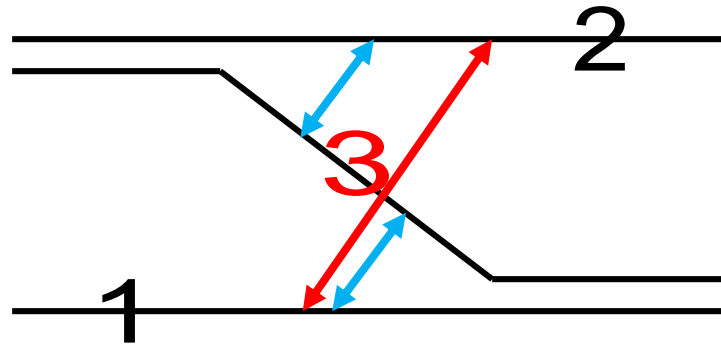
# Efimov-potential as a phenomenological form of GPT-potential in 3-body system

For the 3rd particle transfer:

A)  $r_{23} = r_2 - r_3 = 0$  or  $r_{31} = r_3 - r_1 = 0$

$$V_e(r_1, r_2, r_3) = \frac{V_{e0} a_e^2}{r_{12}^2 + r_{23}^2 + r_{31}^2 + a_e^2} \Rightarrow \frac{V_{e0} a_e^2}{r_{12}^2 + a_e^2}$$

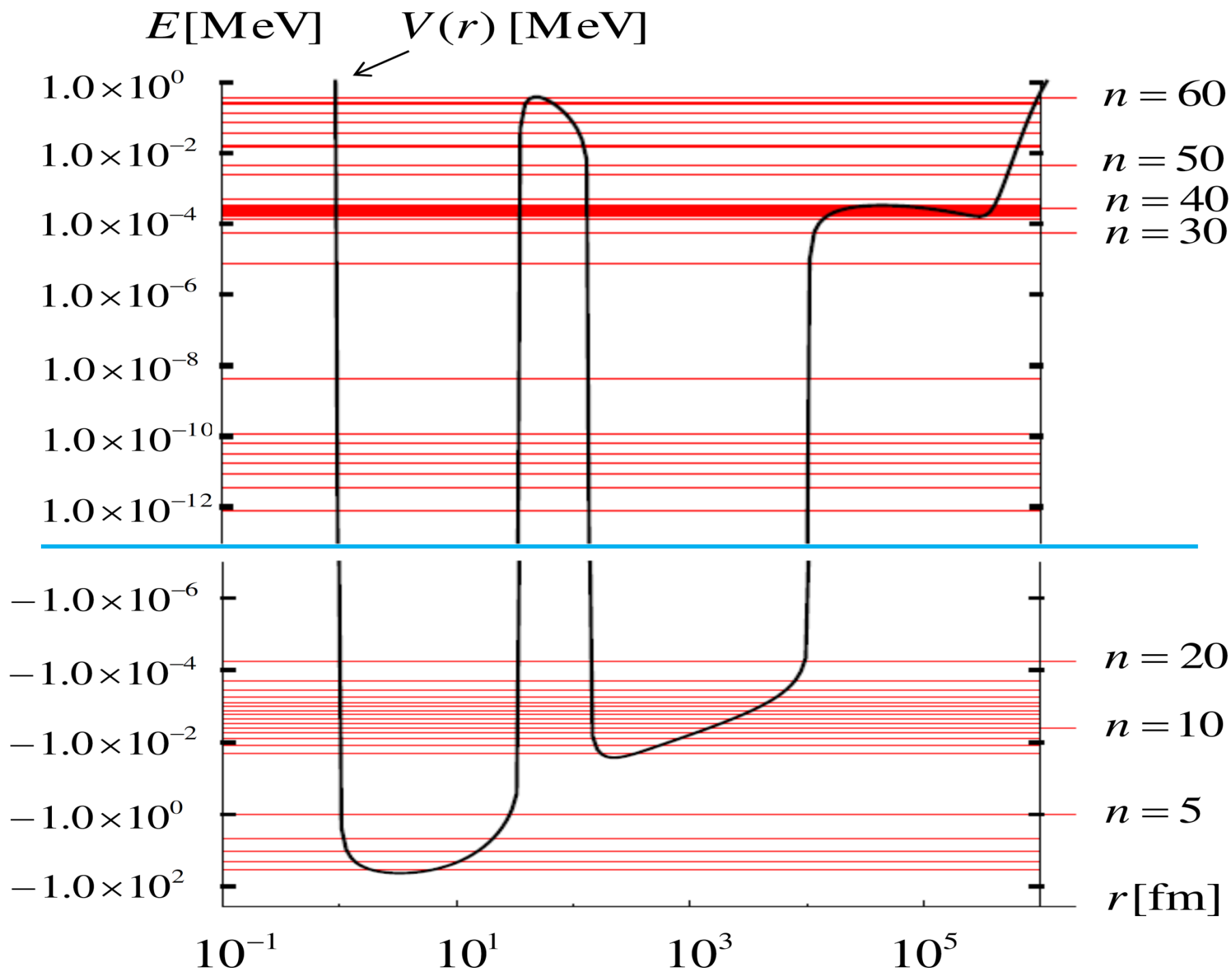
three - body long range (two - body long range pot. = 0)



B)  $r_{12} = r_1 - r_2 = 0$

$$V_e(r_1, r_2, r_3) = \frac{V_{e0} a_e^2}{r_{12}^2 + r_{23}^2 + r_{31}^2 + a_e^2} \Rightarrow \frac{V_{e0} a_e^2}{2r_{23}^2 + a_e^2} = \frac{V_{e0} a_e^2}{2r_{31}^2 + a_e^2}$$

two - body long range (three - body long range pot. = 0)

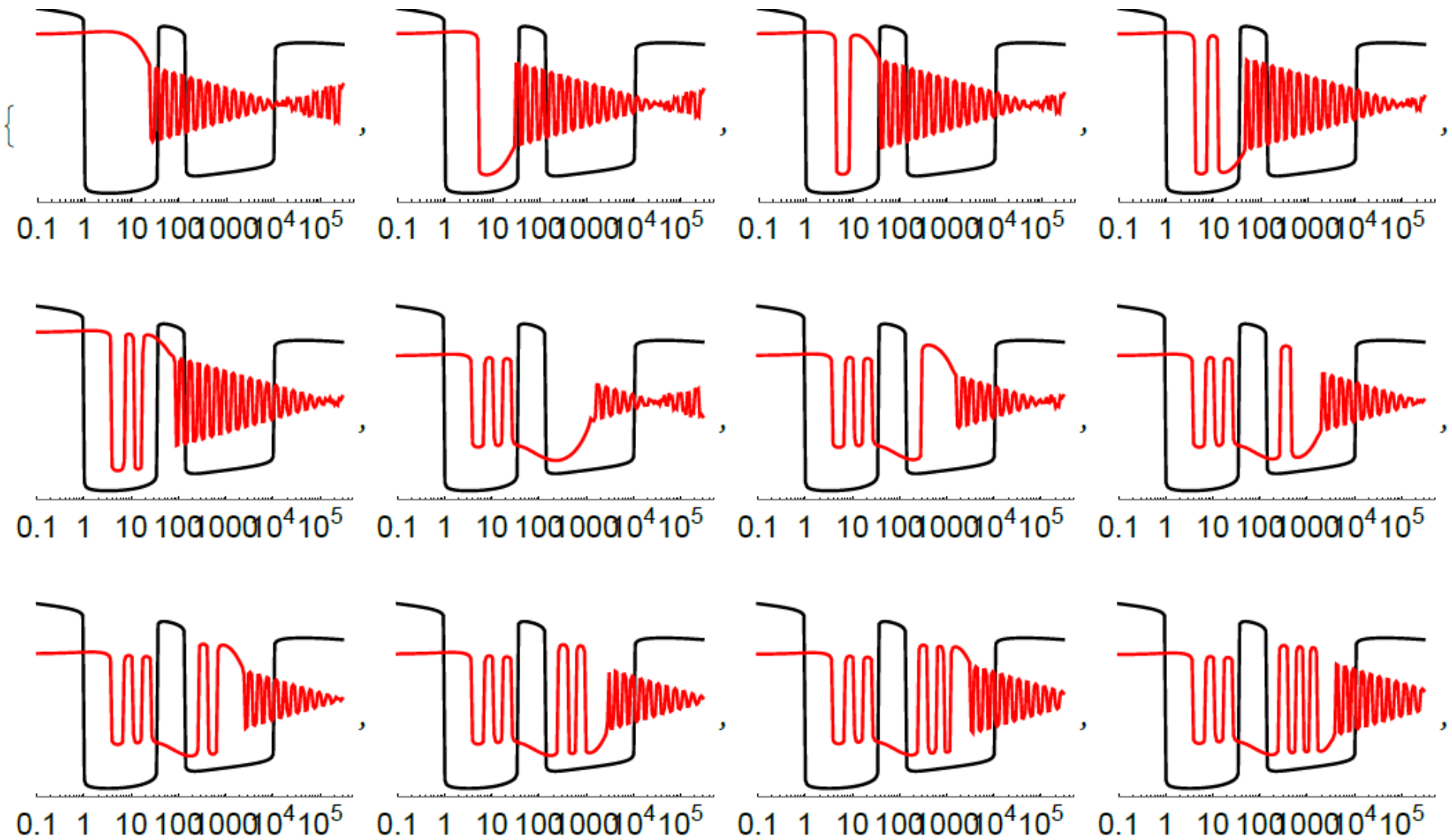


The **wave function overlap value (WFO:  $W_{n,m}$ )**  
between

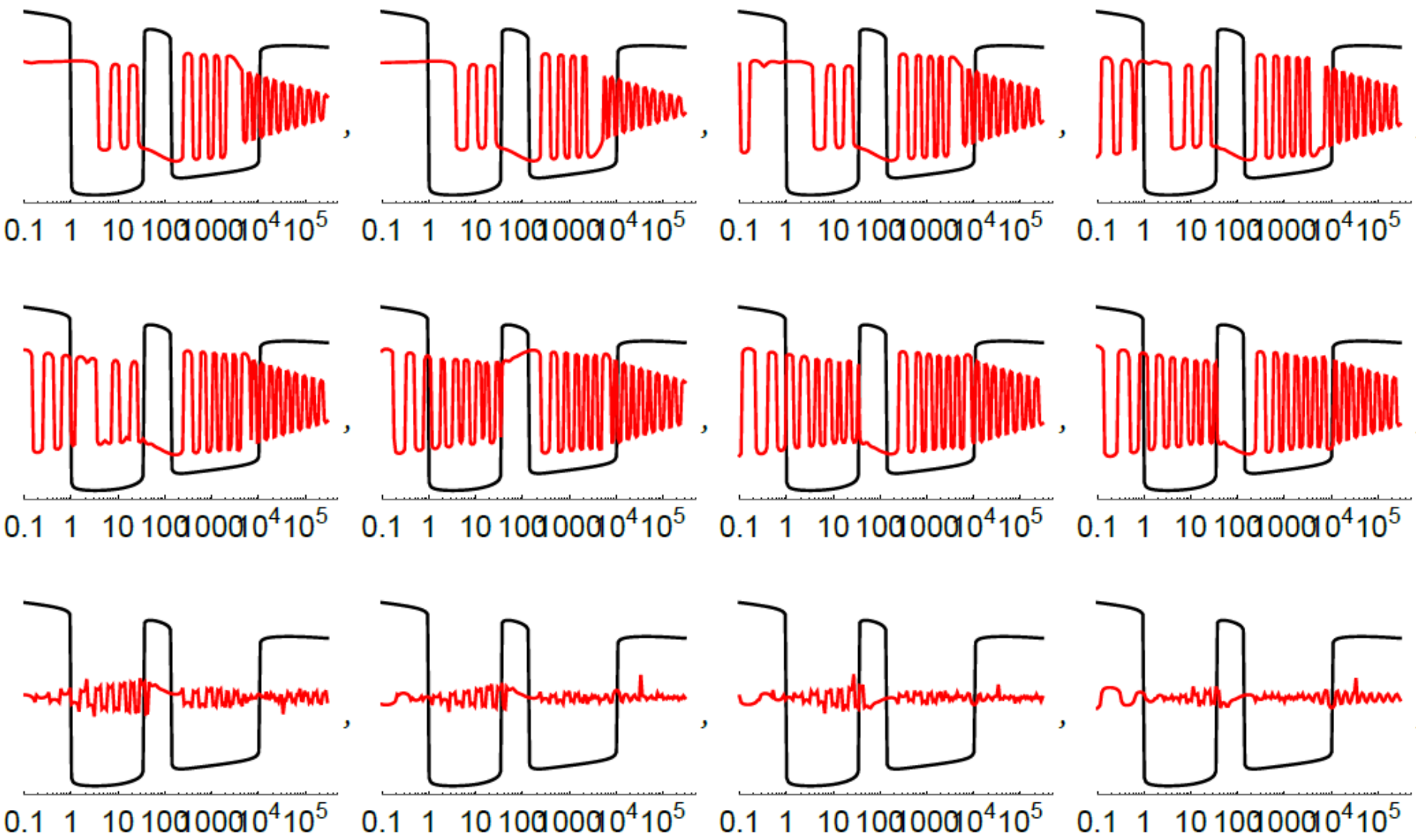
- 1) the **La highest nuclear excited state** with the quantum number  $n = 5$ ,
- 2) and the **lowest  $\text{CsD}_2$  quasi molecular states** is of **critical importance** for the existence of the **electro-magnetic (EM) transition** in the  $\text{Cs}(2d,\gamma)\text{La}$  reaction.



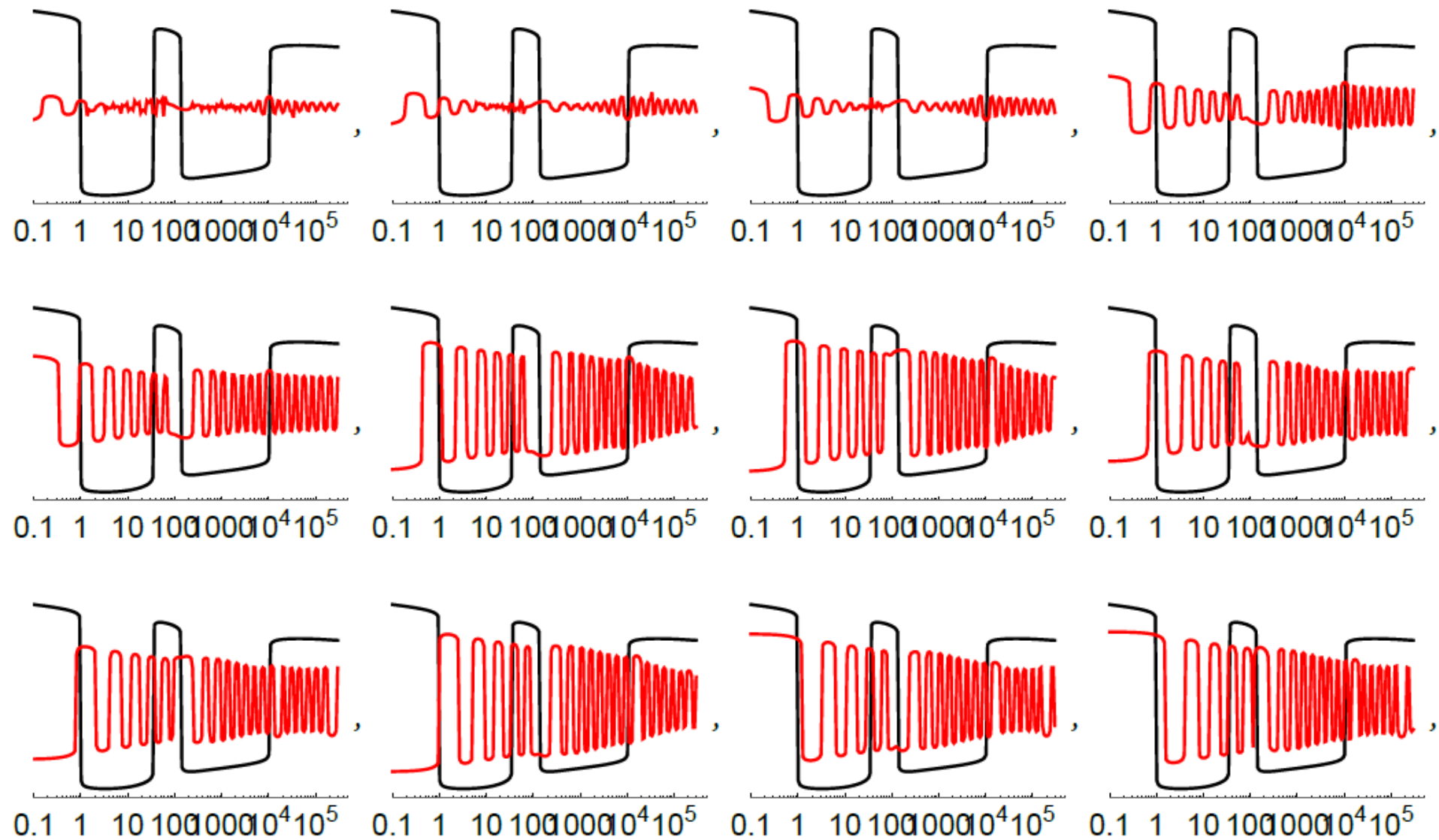
$n = 1 \sim 12$



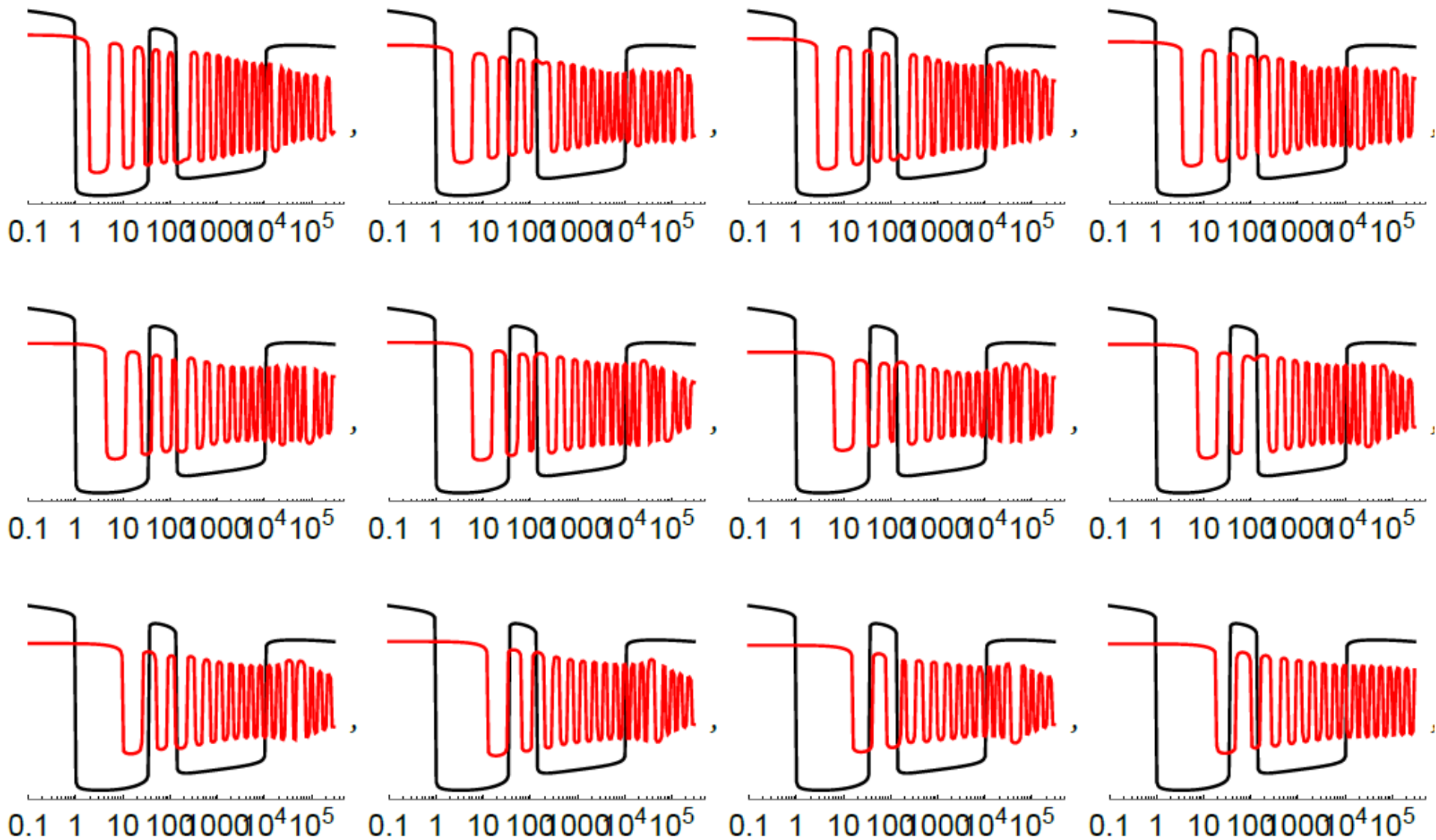
$n = 13 \sim 24$



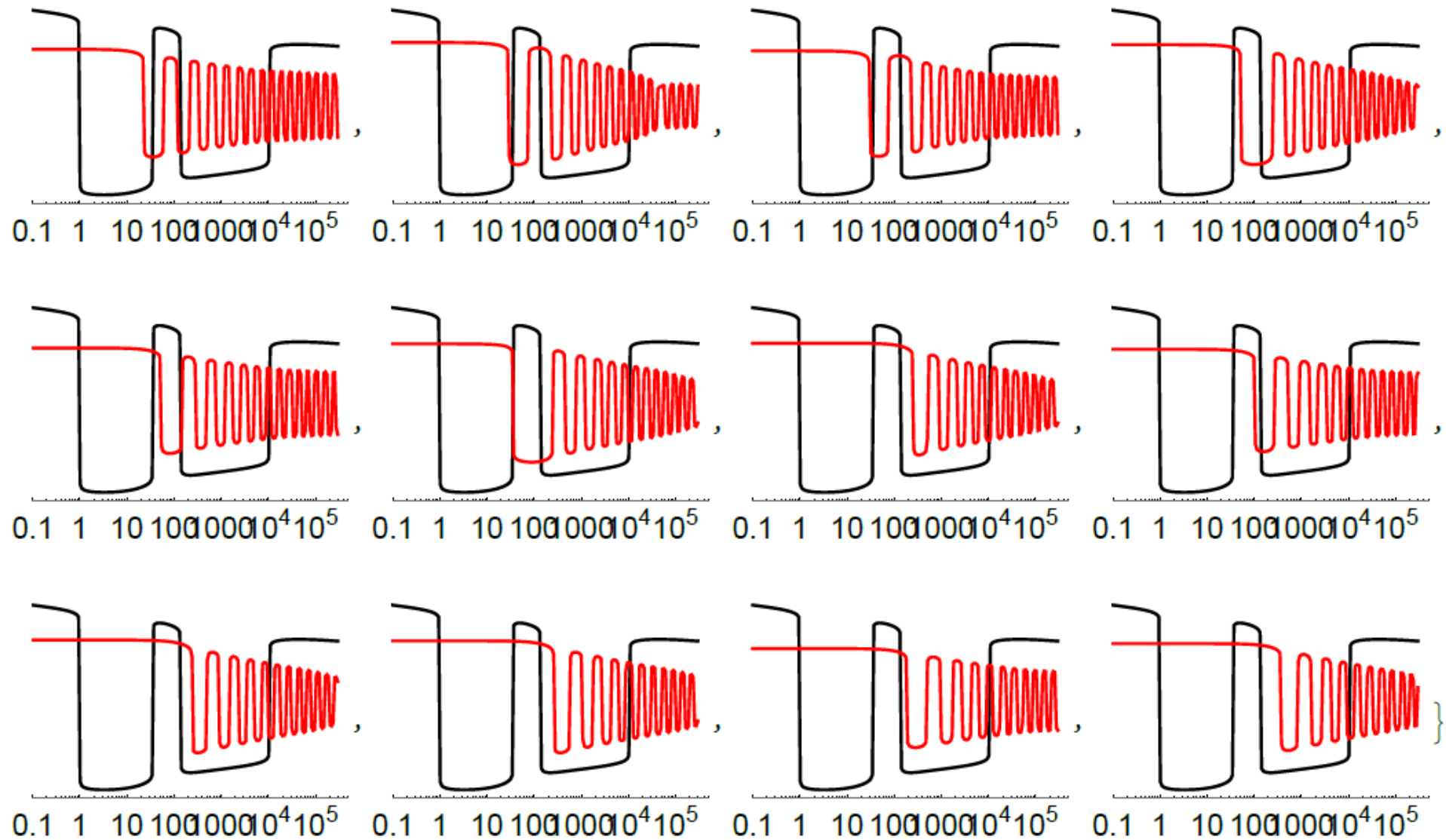
$n = 25 \sim 36$



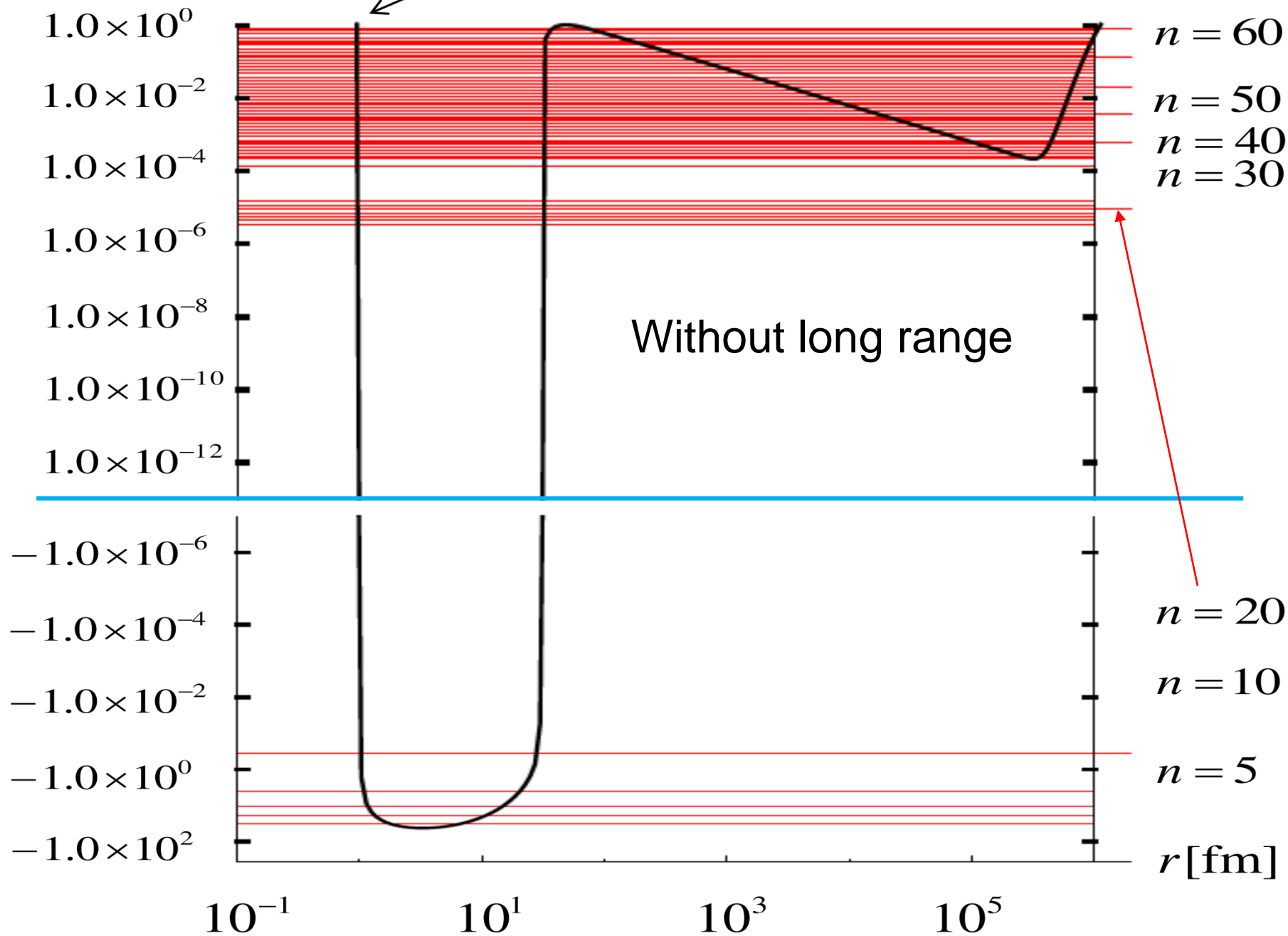
$n = 37 \sim 48$



$n = 49 \sim 60$

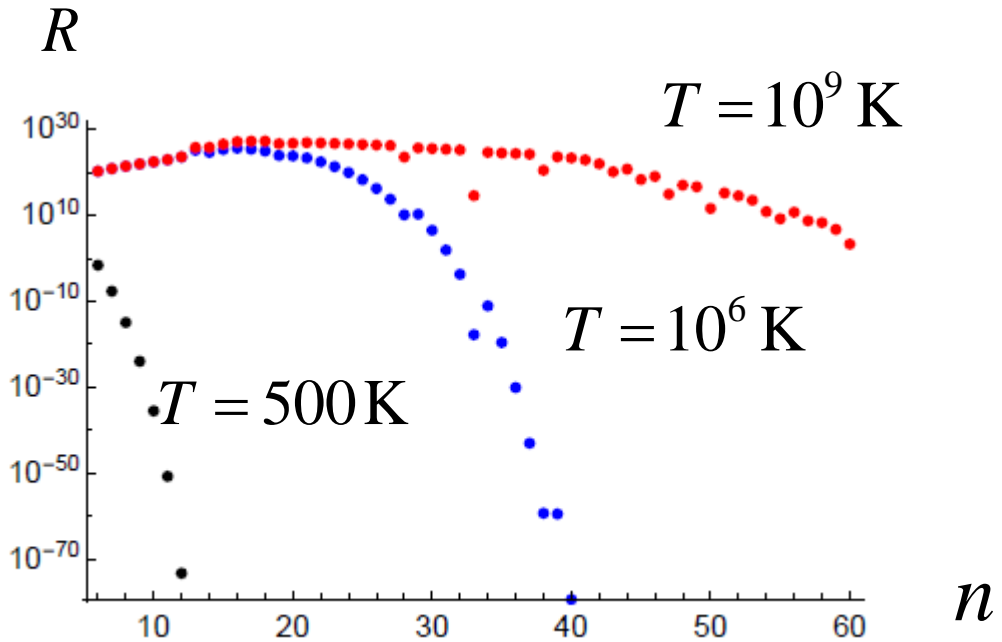
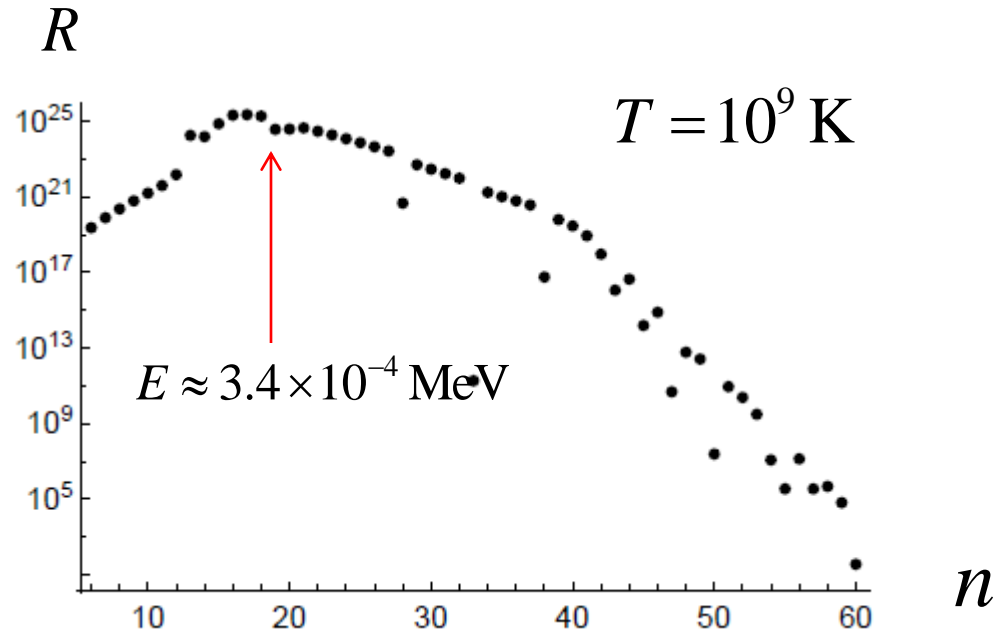


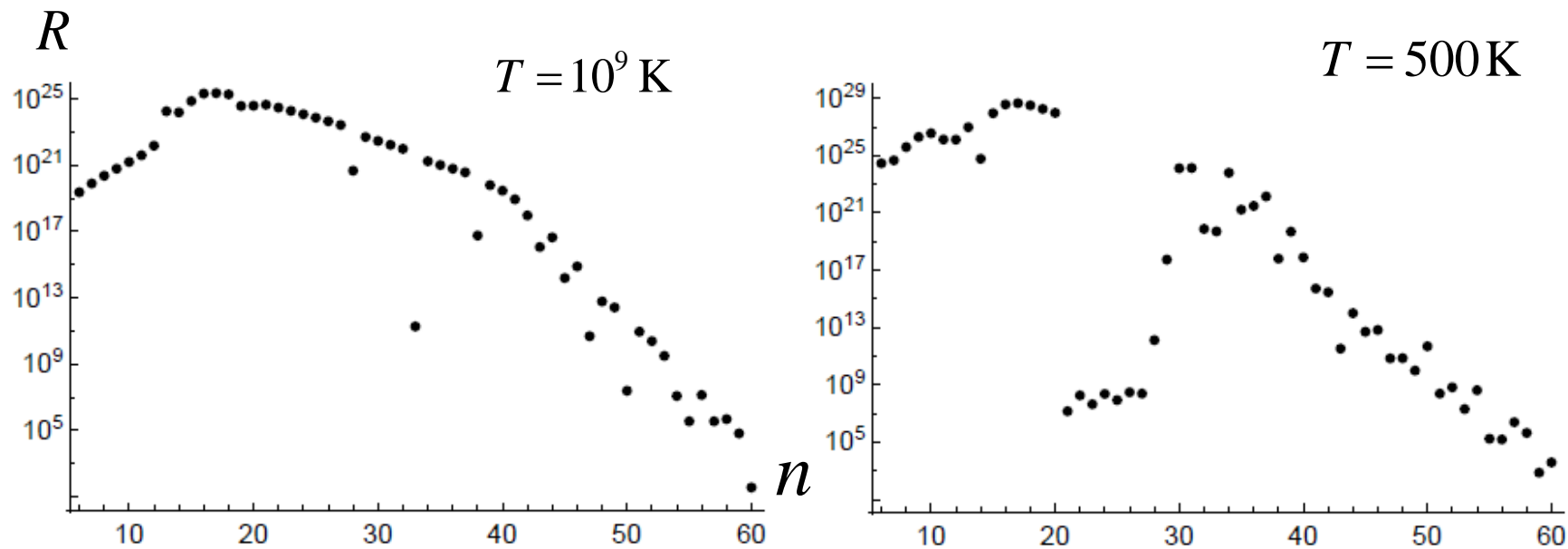
$E$  [MeV]       $V(r)$  [MeV]



Short range  
Nuclear potential

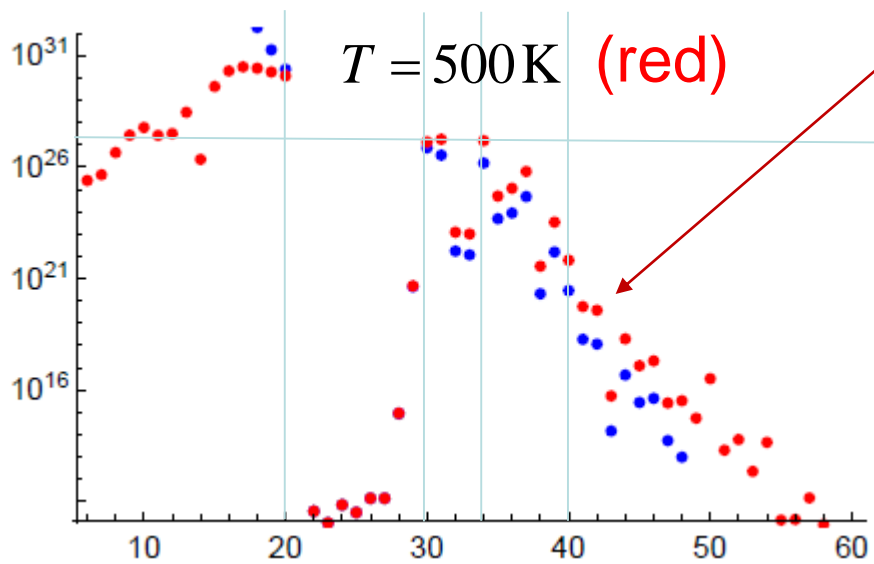
$R$ : transition rate





Short range

With long range





- Transition probability from  $|\psi_i\rangle$  to  $|\psi_f\rangle$  by the spontaneous emission in the vacume

### E1- transition

$$W_{i \rightarrow f}^{E1}(E_i, E_f) = \frac{(E_i - E_f)^3}{3\pi\epsilon_0 h_b^4 c^3} \sum_{k=1}^3 \left| \langle \Psi_f | Z_k e \vec{r}_k | \Psi_i \rangle \right|^2 = \frac{4(E_i - E_f)^3}{3h_b^3 c^2} \left( \frac{1}{4\pi\epsilon_0 h_b c} \right) \sum_{k=1}^3 \left| \langle \Psi_f | Z_k e \vec{r}_k | \Psi_i \rangle \right|^2$$

$$= \left\{ \begin{array}{l} \frac{4(E_i - E_f)^3}{3h_b^3 c^2} \alpha \sum_{k=1}^3 \left| \langle \Psi_f | Z_k e \vec{r}_k | \Psi_i \rangle \right|^2 \\ \frac{4(E_i - E_f)^3}{3} \alpha \sum_{k=1}^3 \left| \langle \Psi_f | Z_k e \vec{r}_k | \Psi_i \rangle \right|^2 \end{array} \right. \begin{array}{l} \text{cgs unit} \\ \text{Natural unit} \end{array}$$

### E2-transition

$$W_{i \rightarrow f}^{E2}(E_i, E_f) = \frac{1}{20} \frac{4(E_i - E_f)^5}{3\pi\epsilon_0 h_b^6 c^3} \sum_{k=1}^3 \left| \langle \Psi_f | \frac{1}{2} (3z_k^2 - x_k^2 - y_k^2) Z_k e | \Psi_i \rangle \right|^2$$

$$\rightarrow W_{i \rightarrow f}^{E2'} = \frac{1}{20} \frac{4(E_i - E_f)^5}{3\pi\epsilon_0 h_b^6 c^3} \sum_{k=1}^3 \left| \langle \Psi_f | \frac{1}{2} r_k^2 Z_k e | \Psi_i \rangle \right|^2$$

### M1-transition

$$W_{i \rightarrow f}^{M1}(E_i, E_f) = \frac{4(E_i - E_f)^3}{3\pi\epsilon_0 h_b^4 c^3} \sum_{k=1}^3 \left| \langle \Psi_f | \frac{Z_k e g_k}{2m_k} (\vec{L}_k + \vec{S}_k) | \Psi_i \rangle \right|^2$$

$g_k$  : gyromagnetic ration of nucleus

- transition time

$$\tau_{i \rightarrow f} = 1/W_{i \rightarrow f}$$

• Let us obtain the transition probability from  $|\psi_i\rangle$  to  $|\psi_f\rangle$  by photon emission from  $\text{CsD}_2\text{Pd}_{12}$  in the thermal equilibrium of temperature  $T$ . The average La number at the energy  $E_i$  and with the temperature  $T$  is given by the Maxwell-Boltzmann distribution;

$$f_{\text{MB}}(E_i, T) = \exp\left[-\frac{E_i}{k_B T}\right] / Z \quad Z = \sum_{j=1} \exp\left[-\frac{E_j}{k_B T}\right] \quad \begin{aligned} k_B &= 1.380649 \times 10^{-23} \text{ J/K} \\ &\approx 8.6171 \times 10^{-8} \text{ MeV/K} \end{aligned}$$

In the radiation field of the thermal equilibrium with the temperature  $T$  and the energy  $E_i$ , the average photon number is given by the Bose-Einstein statistics,

$$f_{\text{BE}}(E_i - E_f) = \frac{1}{\exp\left[\frac{E_i - E_f}{k_B T}\right] - 1} \quad \text{for Black body radiation}$$

Therefore, the transition probability for the unit time, and the unit number of La is given by

$$\frac{dN_{i \rightarrow f}^{\text{E1}}}{dt} = f_{\text{MB}}(E_i, T) \left[ \frac{4(E_i - E_f)^3}{3\pi\epsilon_0 h_b^4 c^3} \sum_{k=1}^3 \left| \langle \Psi_f | Z_k e \vec{r}_k | \Psi_i \rangle \right|^2 + f_{\text{BE}}(E_i - E_f, T) \frac{4(E_i - E_f)^3}{3\pi\epsilon_0 h_b^4 c^3} \sum_{k=1}^3 \left| \langle \Psi_f | Z_k e \vec{r}_k | \Psi_i \rangle \right|^2 \right]$$

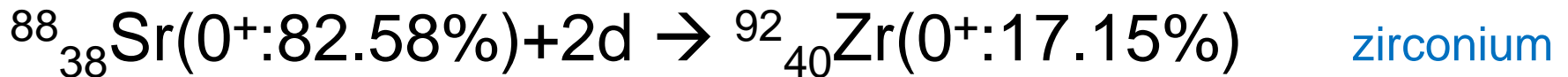
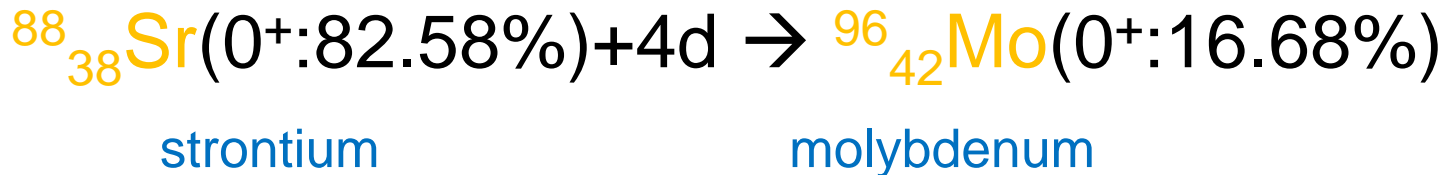
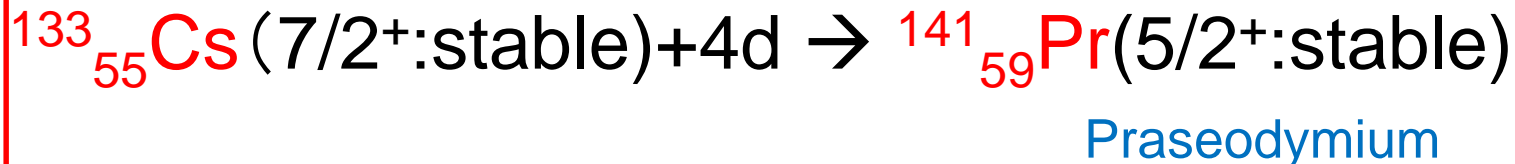
Spontaneous emission (with the particle system)      Stimulated emission (with the photon system)

$$= f_{\text{MB}}(E_i, T) \left[ W_{ij}^{\text{E1}}(E_i, E_f) + f_{\text{BE}}(E_i - E_f, T) W_{ij}^{\text{E1}}(E_i, E_f) \right] = \frac{W_{ij}^{\text{E1}}(E_i, E_f) / Z}{\exp\left[\frac{E_i}{k_B T}\right] - \exp\left[\frac{E_f}{k_B T}\right]}$$

E2, M1 transitions as well

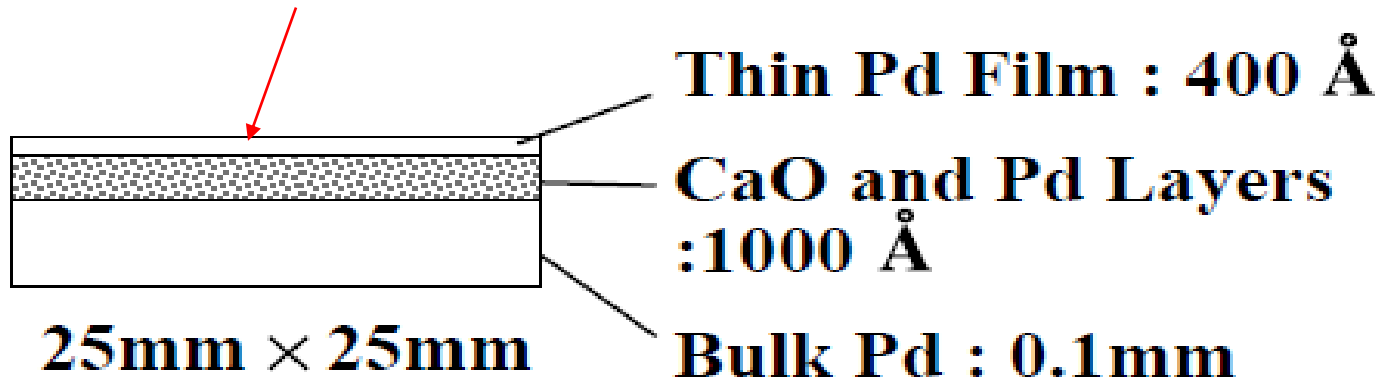
# Recent Experimental Results:

By Iwamura et al. (MHI), (2002)



Hioki et al, Toyota-Nagoya univ. group confirmed  
(2013)

**Cs planting**



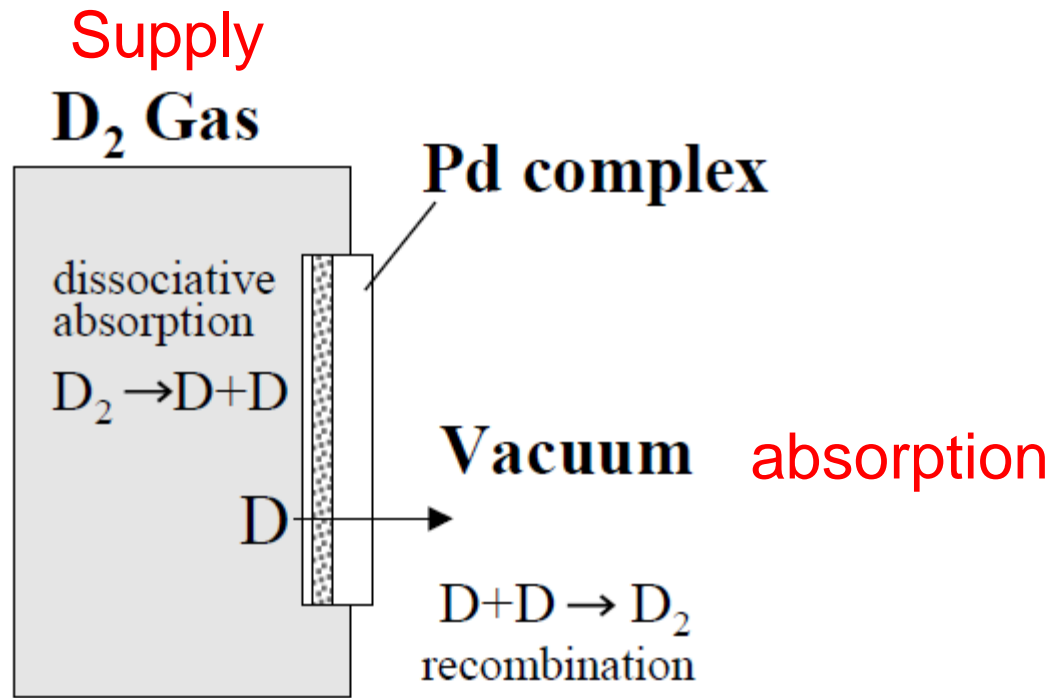
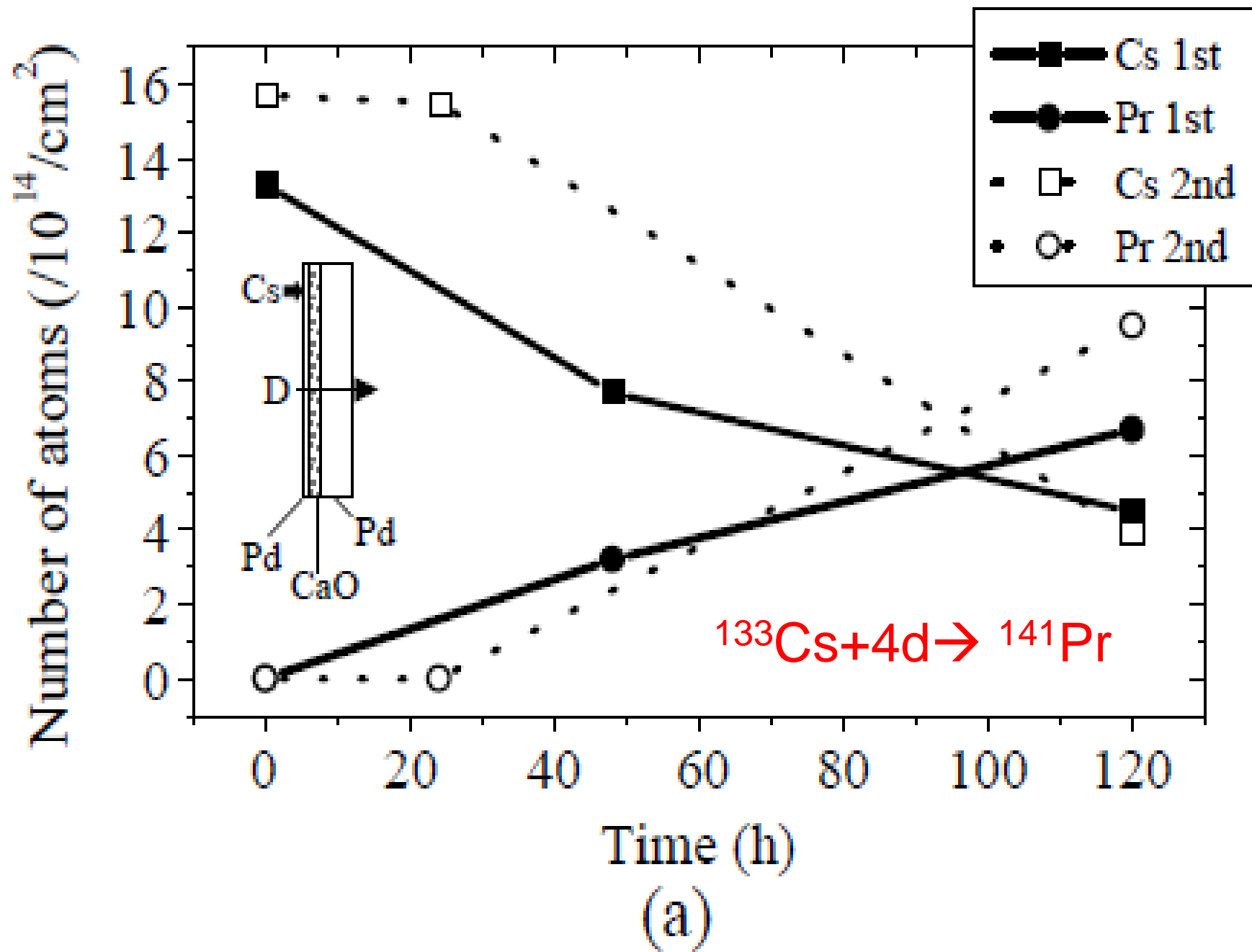
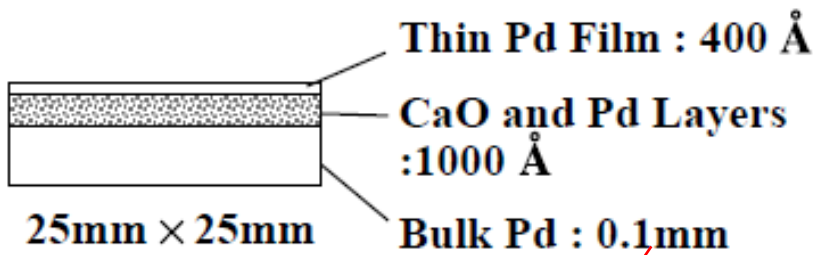


Fig. 1. D<sub>2</sub> gas permeation through the Pd complex.





$$n = 1.4 \times 10^{15} / \text{cm}^2$$

$$T = 343\text{K} \approx 70^\circ\text{C}$$

Transition Probability for:



1) No long range & electron-ion pot.

$$\sum_{i=6}^{n_{\max}} \sum_{f=1}^5 \frac{n}{100} \frac{dN_{i \rightarrow f}^{E2'}}{dt} \times 120 \times 3600 \approx \sum_{i=6}^{60} \sum_{f=1}^5 \frac{n}{100} \frac{dN_{i \rightarrow f}^{E2'}}{dt} \times 120 \times 3600 \approx 7.1 \times 10^7 / \text{cm}^2 \sim \frac{7 \times 10^{14}}{73 \times 10^8} \approx 10^5 \text{ y}$$

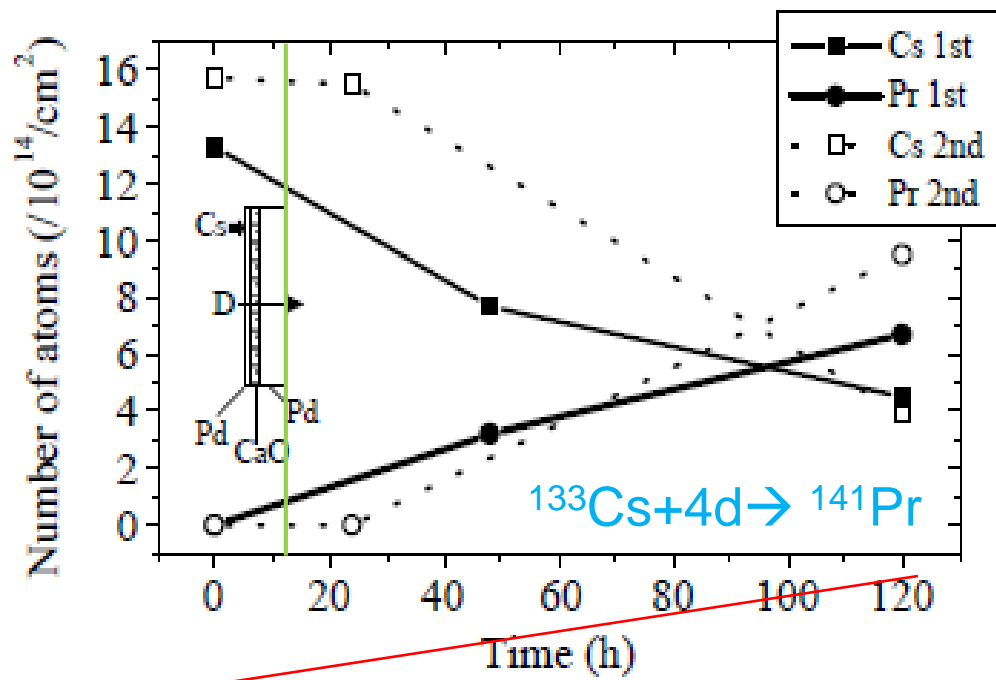
2) With long range, No electron-ion pot.

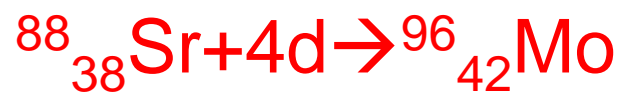
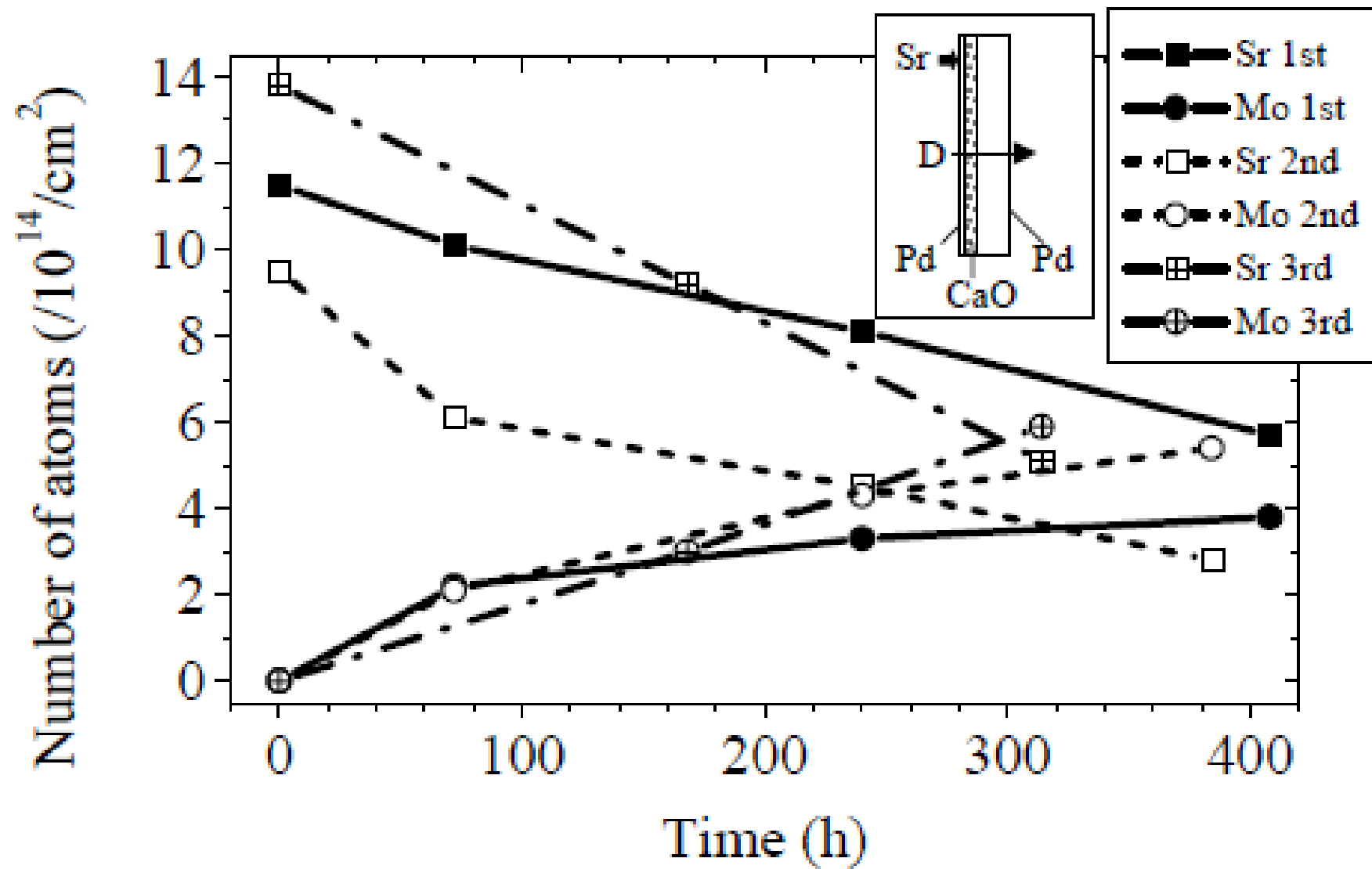
$$W_{i \rightarrow f}^{E2'}(L) = \sum_{i=6}^{n_{\max}} \sum_{f=1}^5 \frac{n}{100} \frac{dN_{i \rightarrow f}^{E2'}}{dt} \times 120 \times 3600 \approx \sum_{i=6}^{60} \sum_{f=1}^5 \frac{n}{100} \frac{dN_{i \rightarrow f}^{E2'}}{dt} \times 120 \times 3600 \approx 1.5 \times 10^{16} / \text{cm}^2$$

Our result is 36 times larger than Experiment.

3) No long range, with electron-ion pot.

$$W_{i \rightarrow f}^{E2'}(S) = \sum_{i=6}^{n_{\max}} \sum_{f=1}^5 \frac{n}{100} \frac{dN_{i \rightarrow f}^{E2'}}{dt} \times 120 \times 3600 \approx \sum_{i=6}^{60} \sum_{f=1}^5 \frac{n}{100} \frac{dN_{i \rightarrow f}^{E2'}}{dt} \times 120 \times 3600 \approx 1.1 \times 10^8 / \text{cm}^2$$





(a)



# Conclusion

1) Wave function overlapping:

$$\frac{W_{56}^L}{W_{56}^S} \approx 10^7$$

Oryu et al. Few Body Syst. (2019) 60 : 42

2) Transition probability for an approximated E2 gives

$$W_{i \rightarrow f}^L \equiv W_{i \rightarrow f}^{E2'}(L) = \sum_{i=6}^{n_{\max}} \sum_{f=1}^5 \frac{n}{100} \frac{dN_{i \rightarrow f}^{E2'}}{dt} \times 120 \times 3600 \approx \underline{1.5 \times 10^{16} / \text{cm}^2}$$

$$W_{i \rightarrow f}^S \equiv W_{i \rightarrow f}^{E2'}(S) = \sum_{i=6}^{n_{\max}} \sum_{f=1}^5 \frac{n}{100} \frac{dN_{i \rightarrow f}^{E2'}}{dt} \times 120 \times 3600 \approx \underline{1.1 \times 10^8 / \text{cm}^2}$$

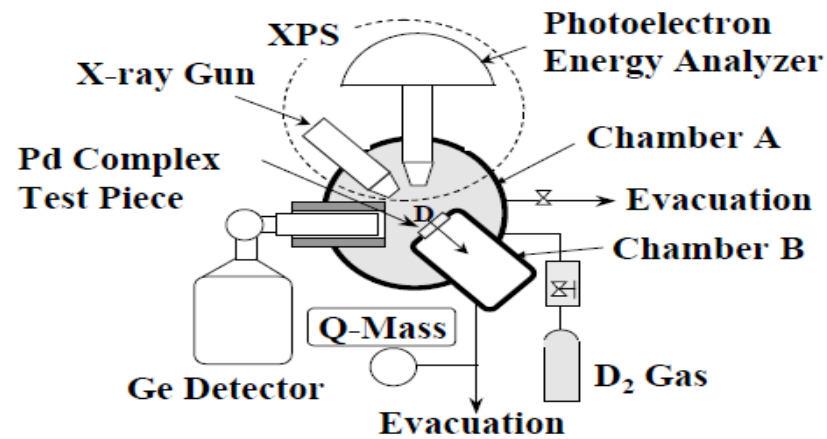
$$\frac{W_{i \rightarrow f}^L}{W_{i \rightarrow f}^S} \sim 10^8$$

- 3) Long Range Potential is essential to obtain the ultra low energy nuclear synthesis.
- 4) The GPT  $1/r^n$ -type potentials are promising for the D-particle transfer potential in D-Cs-D of  $1/r^2$  (or  $1/r^3$ ) – type, while  $D_2$ -transfer in  $D_2$ -Cs- $D_2$  could be  $1/r^3$  (or  $1/r^4$ ) – type potential etc.

- 5) Therefore, pure D-absorption into Pd complex never occur the  $D+D \rightarrow {}^4\text{He}$  fusion, because  $D\text{-Pd}_n$  is not a three-body system but a many-body system, then no GPT potential could be made.
- 6) Our *theoretical* calculation is the first success for the description of ultra low energy nuclear synthesis after the Experimental breakthrough was done.
- 7) As a conclusion, our Few-Body community could contribute to ultra low energy nuclear synthesis by the GPT long range potential.

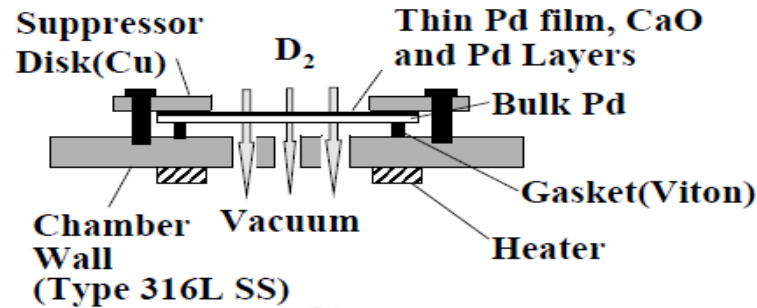
Thank you very much for your attention!



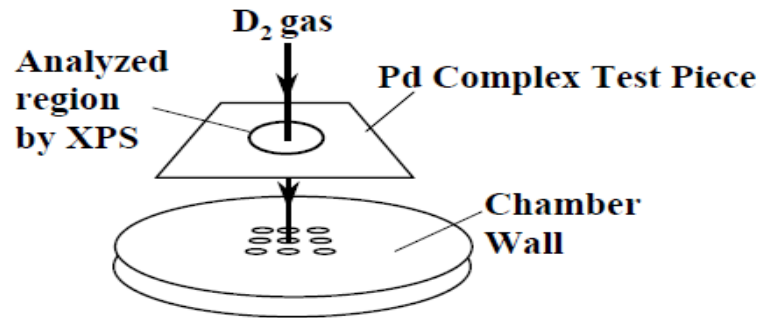


(a)

XPS: X-ray photoelectron spectroscopy



(b)



(c)

Fig. 3. (a) Experimental apparatus, (b) Schematic of test setup in the vicinity of Pd complex test piece, (c) Path of D<sub>2</sub> gas flowing through Pd complex test piece and chamber wall.

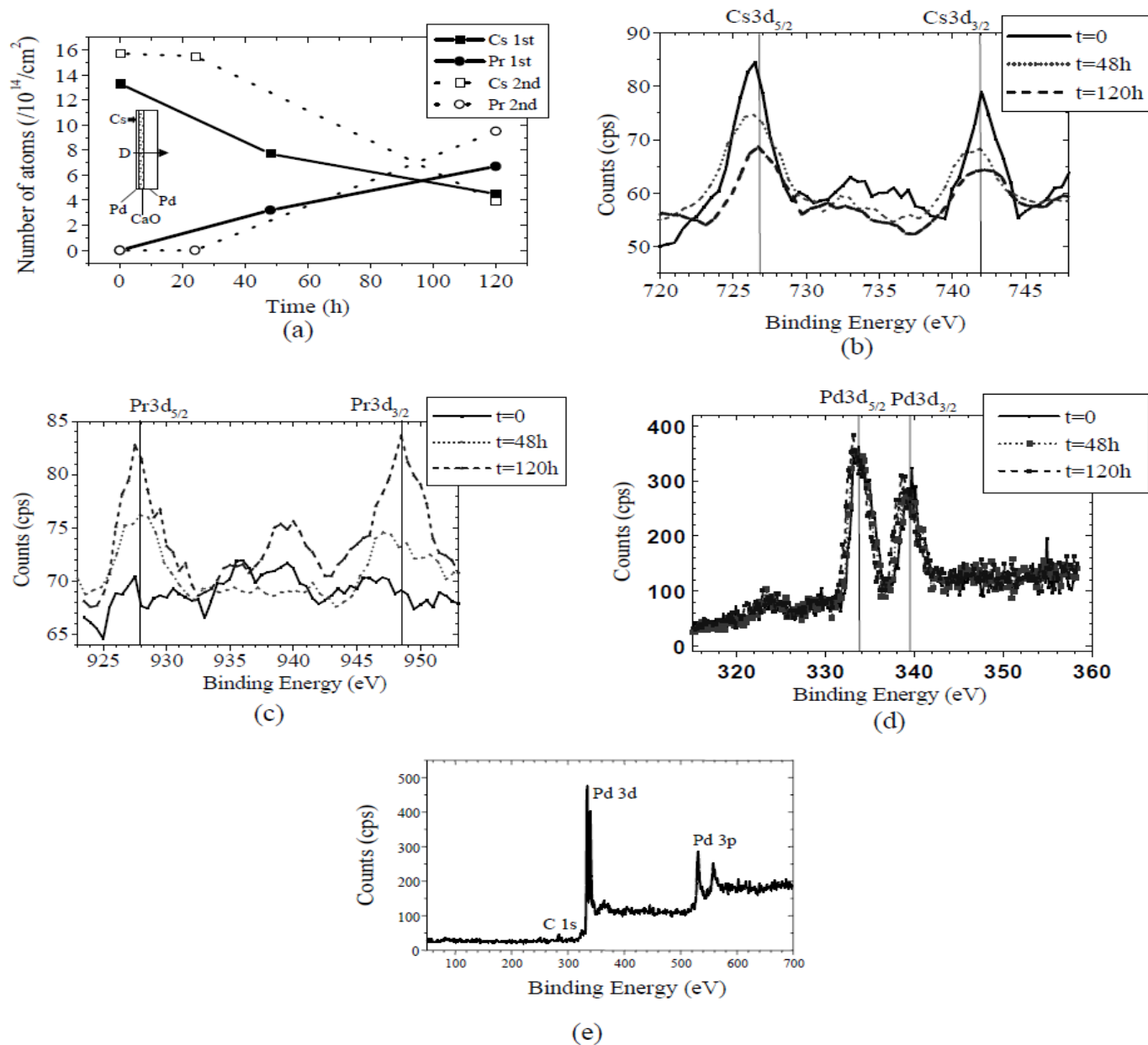


Fig. 4. Experimental results obtained by  $D_2$  gas permeation through Pd complex (Pd/CaO/Pd) deposited with Cs: (a) Time variation in number of Cs and Pr atoms (number of atoms per  $cm^2$ ), (b) XPS spectrum of Cs for experiment run #1, (c) XPS spectrum of Pr for experiment run #1, (d) XPS spectrum of Pd for experiment run #1, (e) Wide-range XPS spectrum for experiment run #1.

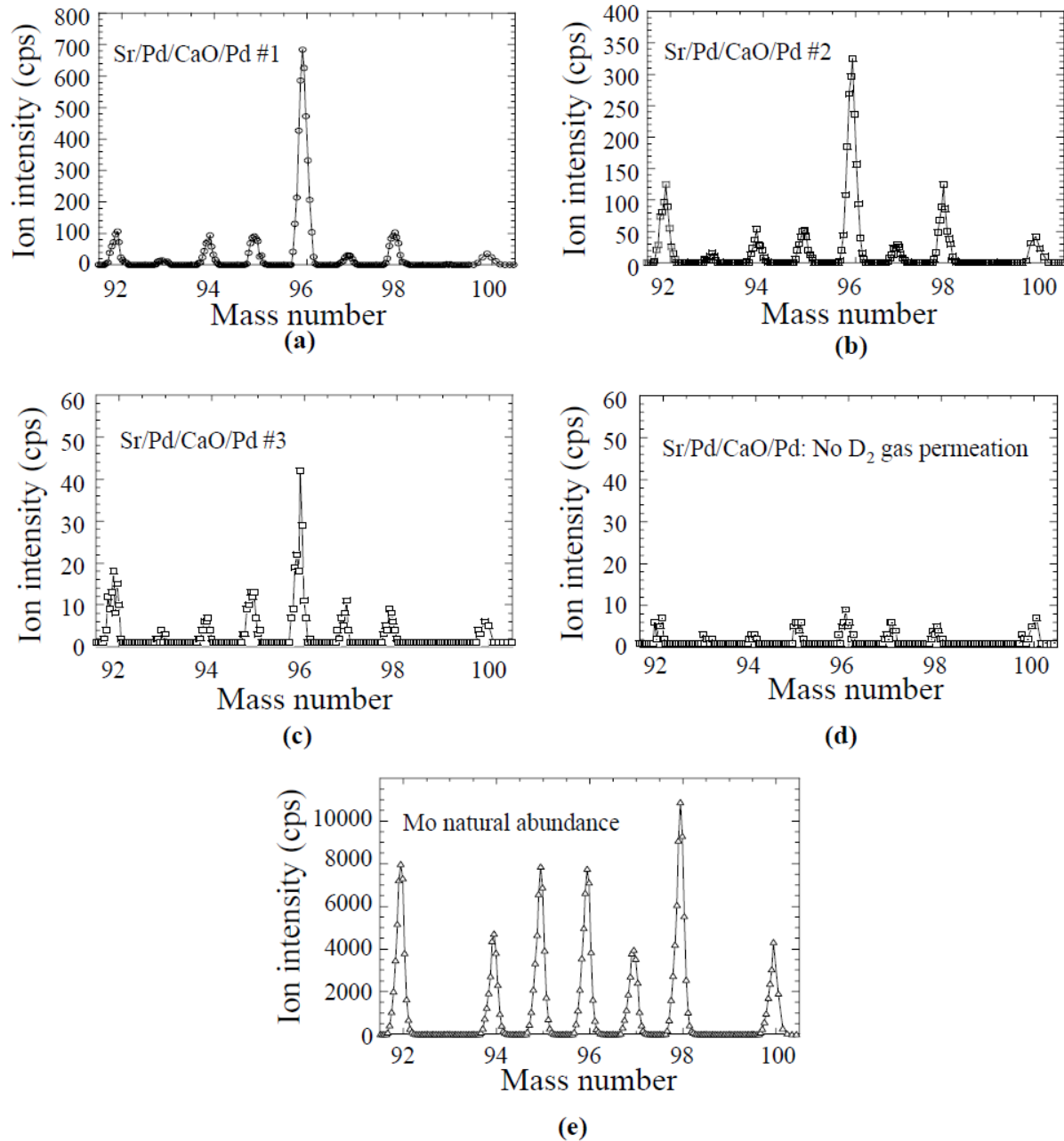
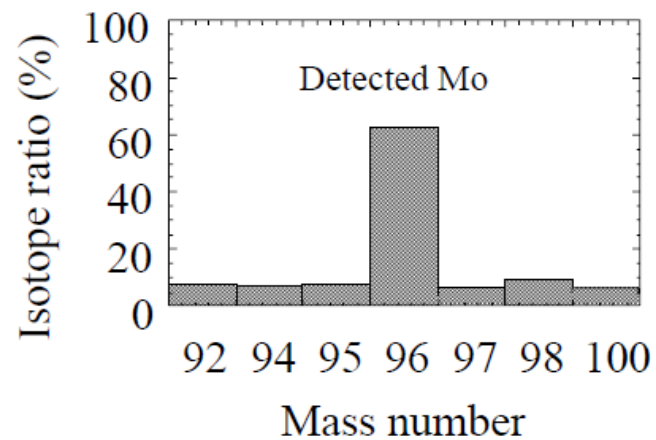
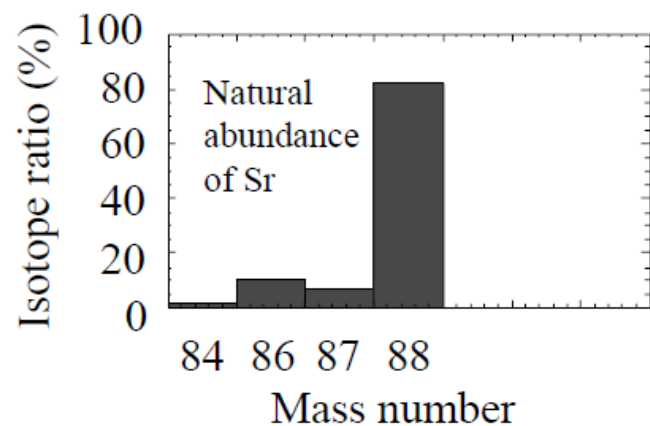


Fig. 9. Anomalous isotopic composition of detected Mo: (a) Isotopic composition of detected Mo for run #1, (b) Isotopic composition of detected Mo for run #2, (c) Isotopic composition of detected Mo for run #3, (d) SIMS analysis for Pd complex test piece with added Sr without D<sub>2</sub> gas permeation, (e) Natural abundance of Mo analyzed by SIMS.





(a)



(b)

Fig. 10. Relationship of mass numbers between given Sr and detected Mo: (a) Isotopic composition of detected Mo, (b) Isotopic composition of given Sr.



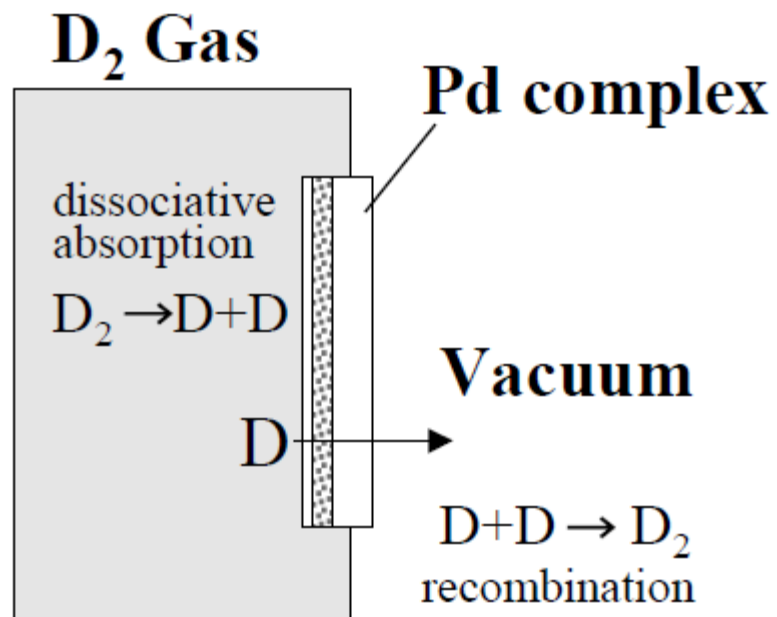
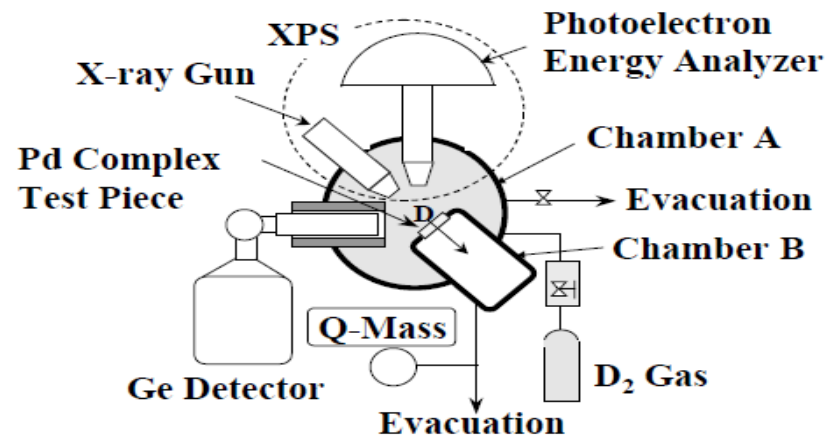
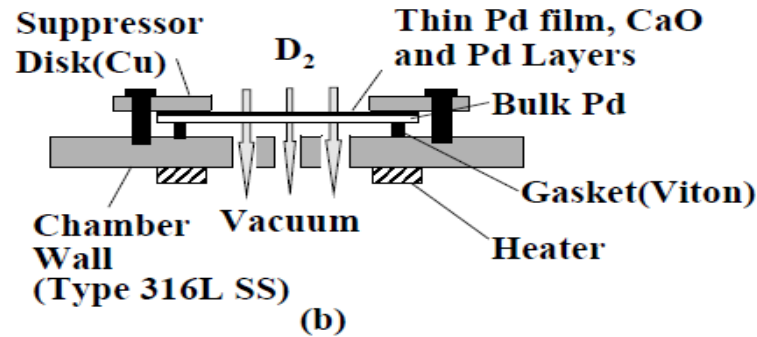


Fig. 1. D<sub>2</sub> gas permeation through the Pd complex.

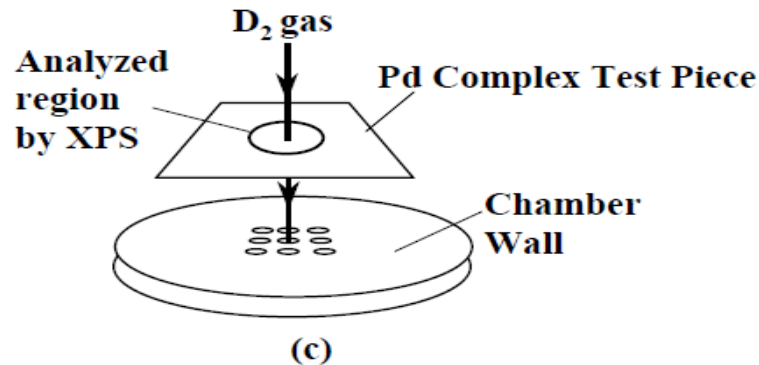


(a)

XPS: X-ray photoelectron spectroscopy



(b)



(c)

Fig. 3. (a) Experimental apparatus, (b) Schematic of test setup in the vicinity of Pd complex test piece, (c) Path of D<sub>2</sub> gas flowing through Pd complex test piece and chamber wall.

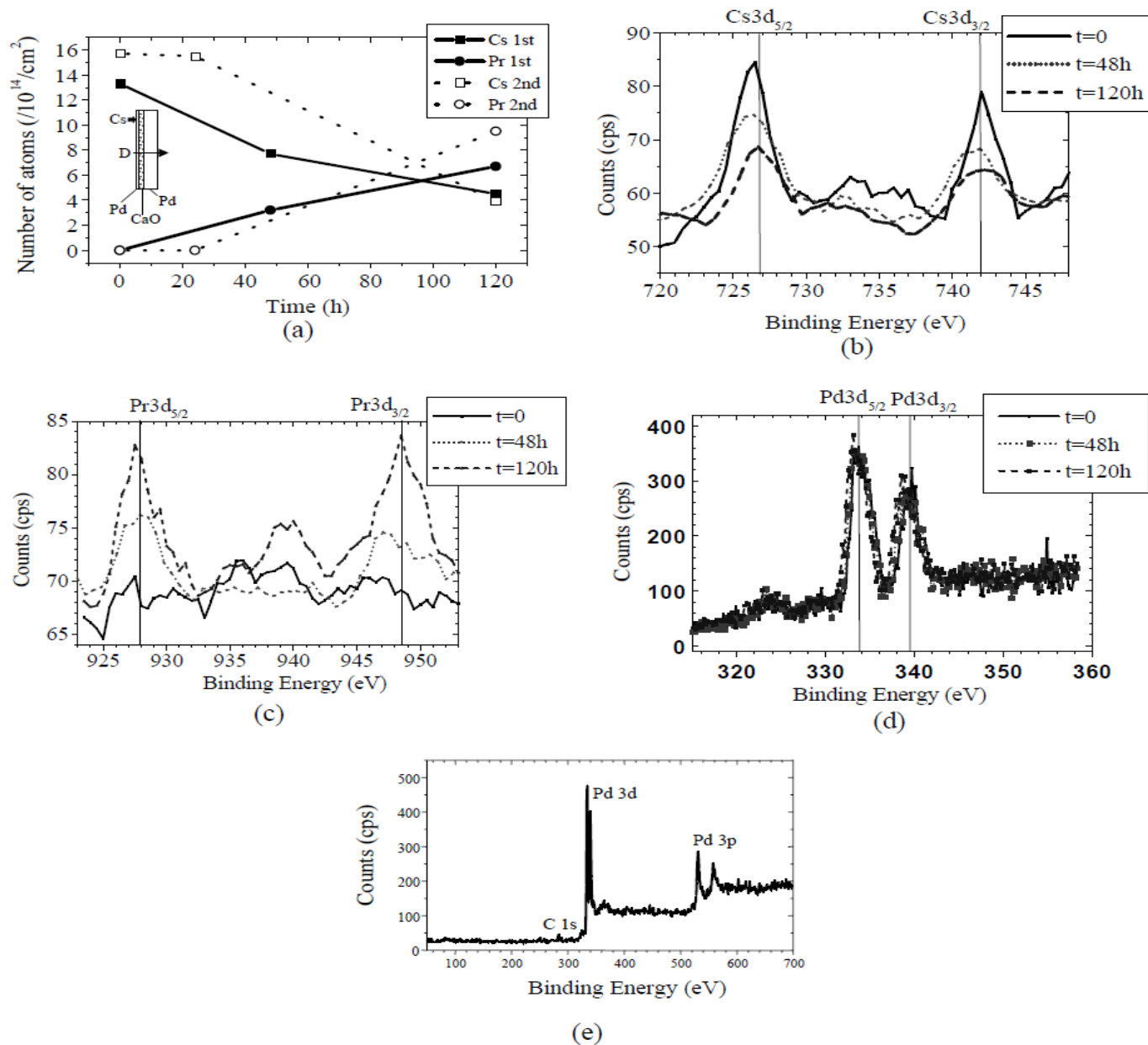


Fig. 4. Experimental results obtained by  $D_2$  gas permeation through Pd complex (Pd/CaO/Pd) deposited with Cs: (a) Time variation in number of Cs and Pr atoms (number of atoms per  $cm^2$ ), (b) XPS spectrum of Cs for experiment run #1, (c) XPS spectrum of Pr for experiment run #1, (d) XPS spectrum of Pd for experiment run #1, (e) Wide-range XPS spectrum for experiment run #1.

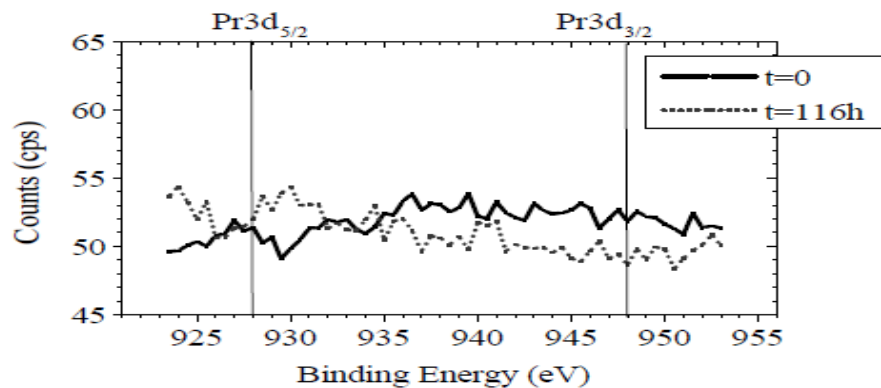
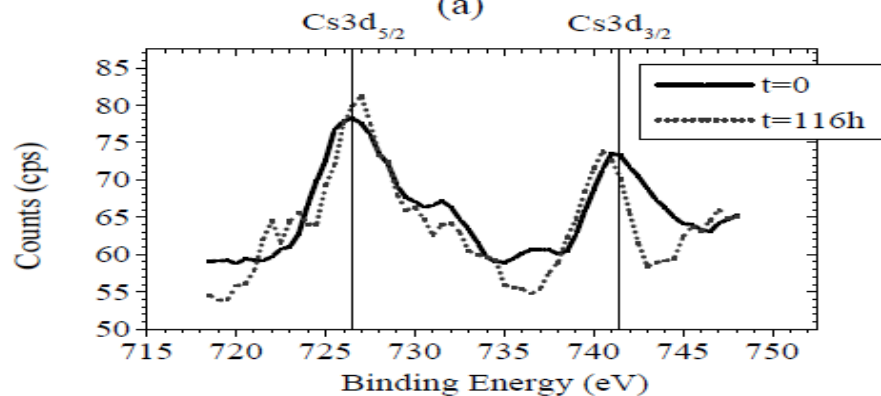
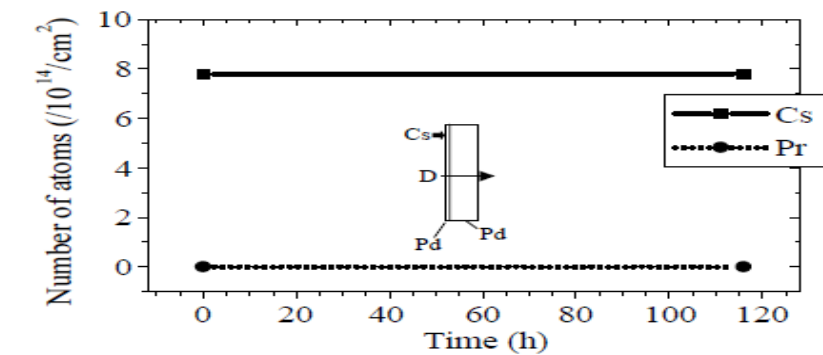


Fig. 5. Experimental results obtained by  $\text{D}_2$  gas permeation through thin film and bulk Pd with added Cs: (a) Time variation in number of Cs and Pr atoms, (b) XPS spectrum of Cs, (c) XPS spectrum of Pr.

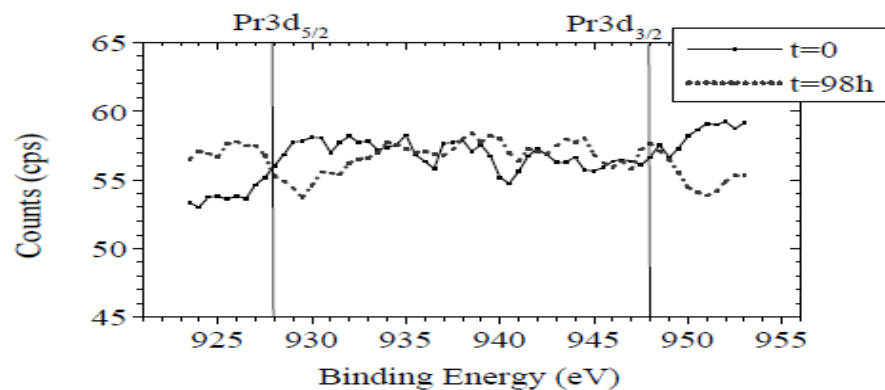
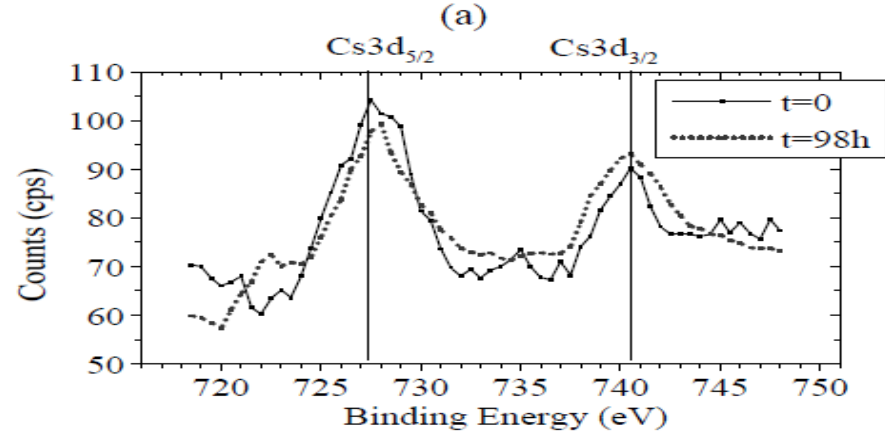
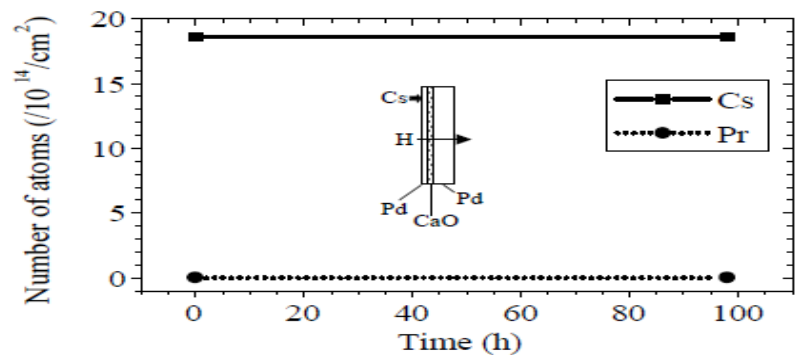


Fig. 6. Experimental results obtained by  $\text{H}_2$  gas permeation through Pd complex (Pd/CaO/Pd) with added Cs: (a) Time variation in number of Cs and Pr atoms, (b) XPS spectrum of Cs, (c) XPS spectrum of Pr.

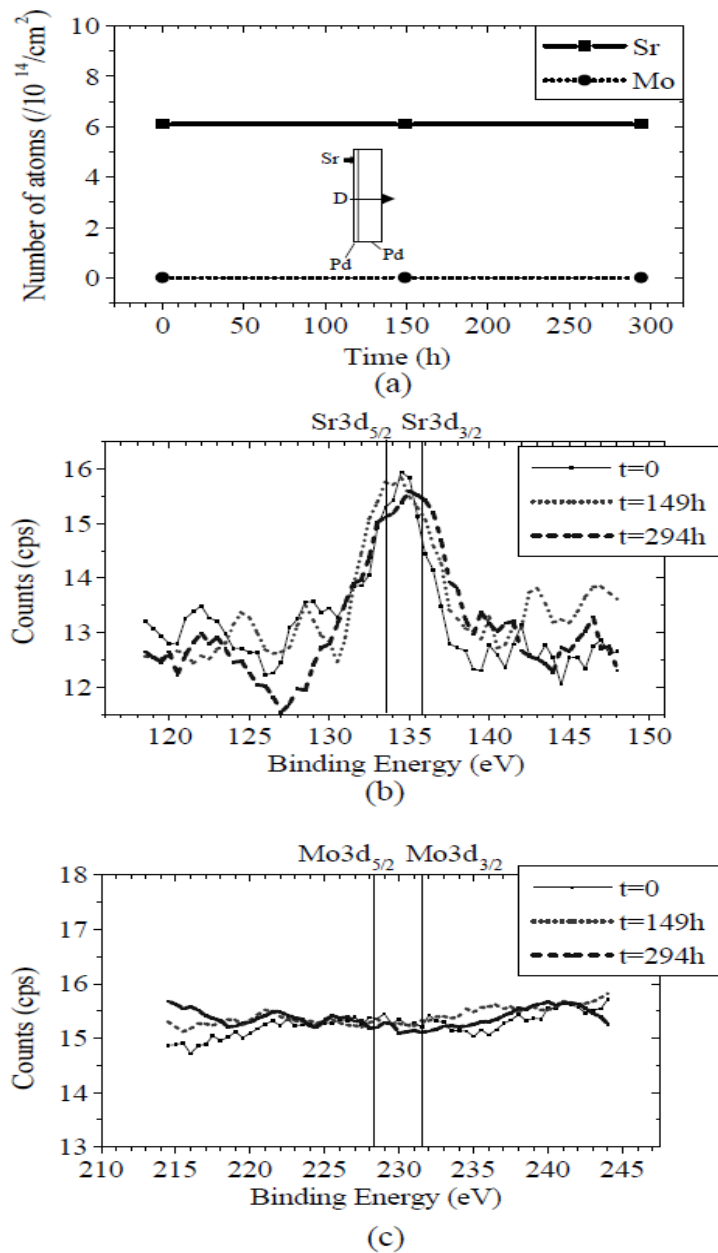


Fig. 8. Experimental results obtained by D<sub>2</sub> gas permeation through thin film and bulk Pd deposited with Sr: (a) Time variation in number of Sr and Mo atoms, (b) XPS spectrum of Sr, (c) XPS spectrum of Mo.

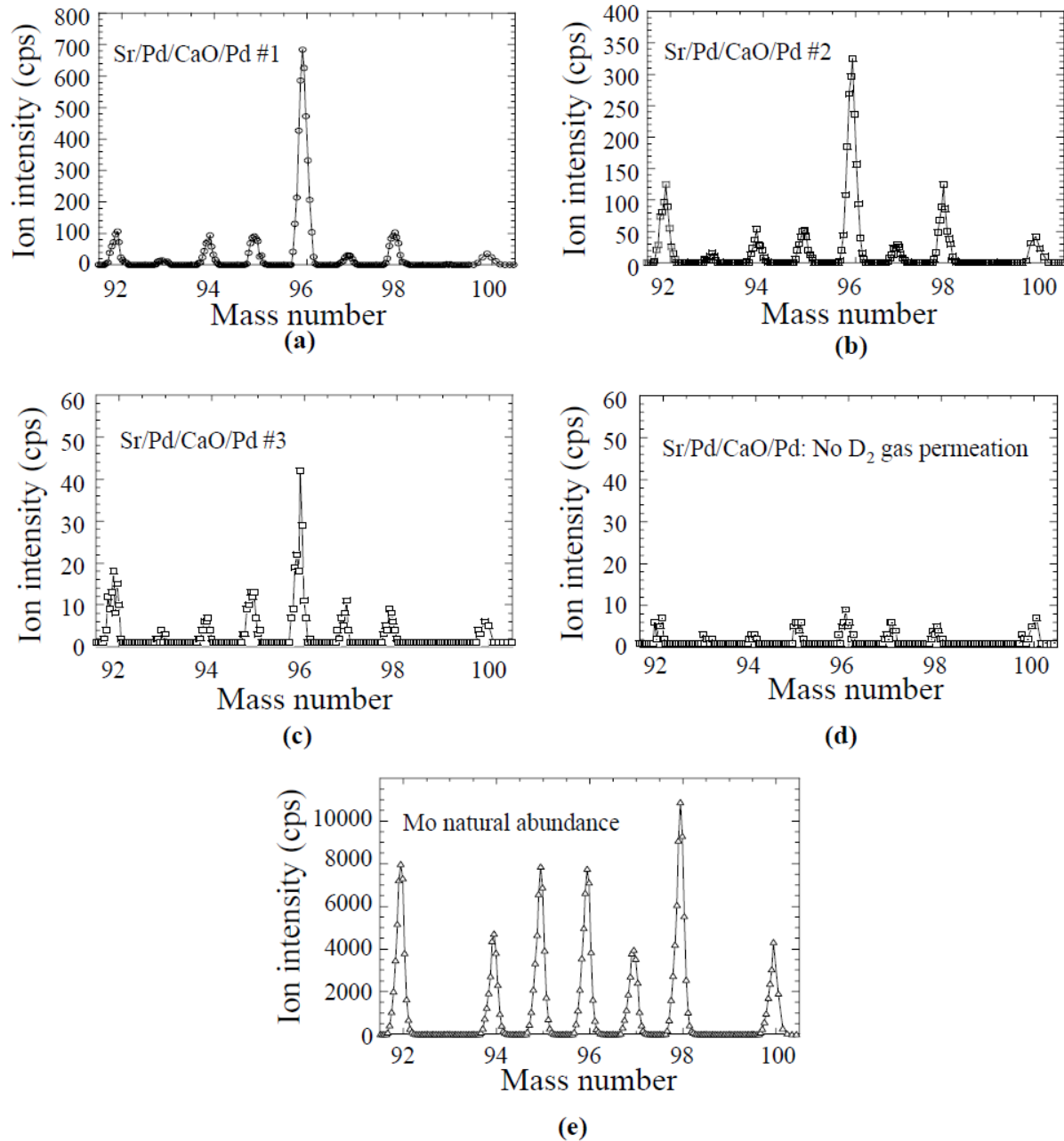
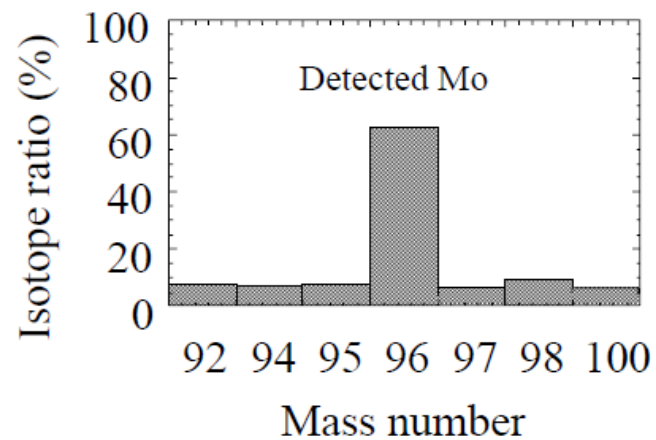
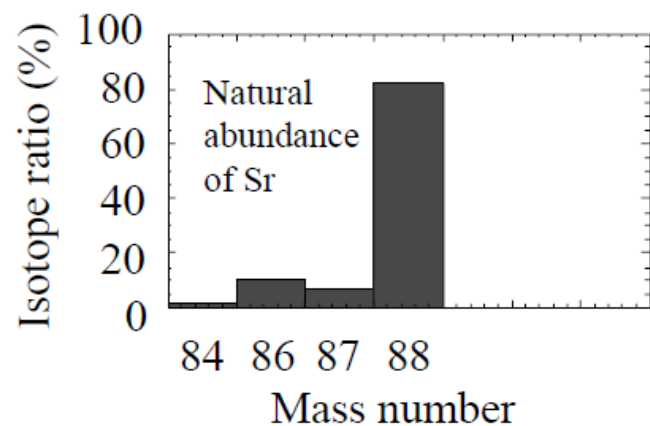


Fig. 9. Anomalous isotopic composition of detected Mo: (a) Isotopic composition of detected Mo for run #1, (b) Isotopic composition of detected Mo for run #2, (c) Isotopic composition of detected Mo for run #3, (d) SIMS analysis for Pd complex test piece with added Sr without D<sub>2</sub> gas permeation, (e) Natural abundance of Mo analyzed by SIMS.



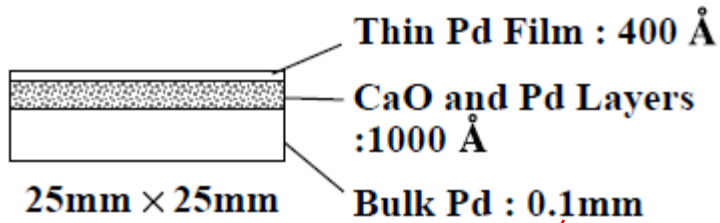


(a)



(b)

Fig. 10. Relationship of mass numbers between given Sr and detected Mo: (a) Isotopic composition of detected Mo, (b) Isotopic composition of given Sr.



$$n = 1.4 \times 10^{15} / \text{cm}^2$$

$$T = 343\text{K} \approx 70^\circ\text{C}$$

- No long range pot.      No electron-ion pot.

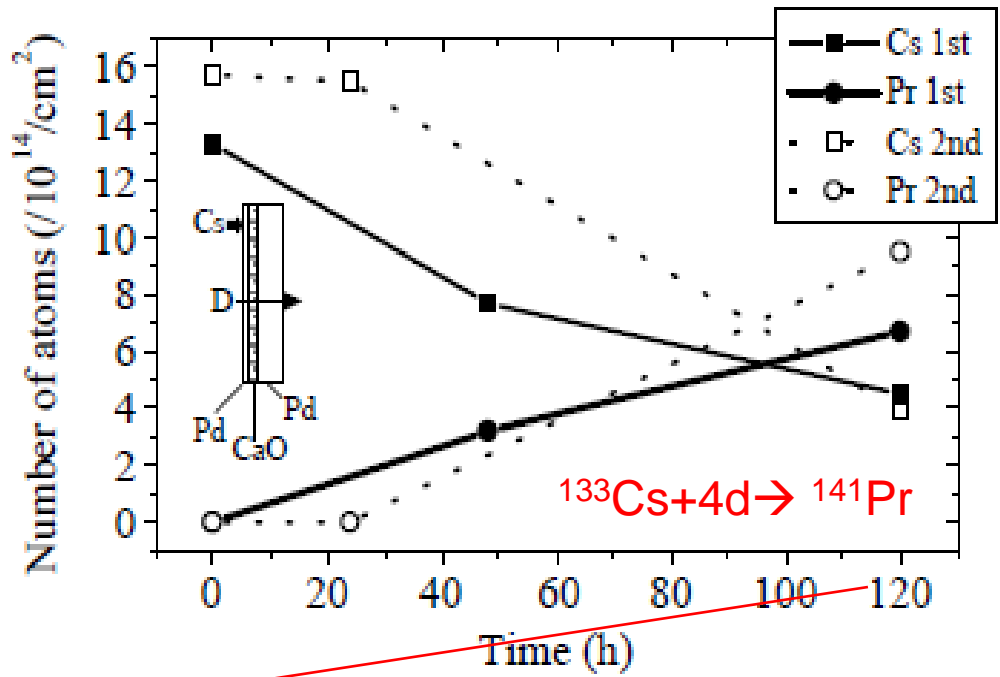
$$\sum_{i=6}^{n_{\max}} \sum_{f=1}^5 \frac{n}{100} \frac{dN_{i \rightarrow f}^{E2'}}{dt} \times 120 \times 3600 \approx \sum_{i=6}^{60} \sum_{f=1}^5 \frac{n}{100} \frac{dN_{i \rightarrow f}^{E2'}}{dt} \times 120 \times 3600 \approx 7.1 \times 10^7 / \text{cm}^2$$

- With long range      No electro-ion pot.

$$\sum_{i=6}^{n_{\max}} \sum_{f=1}^5 \frac{n}{100} \frac{dN_{i \rightarrow f}^{E2'}}{dt} \times 120 \times 3600 \approx \sum_{i=6}^{60} \sum_{f=1}^5 \frac{n}{100} \frac{dN_{i \rightarrow f}^{E2'}}{dt} \times 120 \times 3600 \approx 1.5 \times 10^{16} / \text{cm}^2$$

- No long range pot.      With electron-ion pot.

$$\sum_{i=6}^{n_{\max}} \sum_{f=1}^5 \frac{n}{100} \frac{dN_{i \rightarrow f}^{E2'}}{dt} \times 120 \times 3600 \approx \sum_{i=6}^{60} \sum_{f=1}^5 \frac{n}{100} \frac{dN_{i \rightarrow f}^{E2'}}{dt} \times 120 \times 3600 \approx 1.1 \times 10^8 / \text{cm}^2 \sim \frac{7 \times 10^{14}}{73 \times 10^8} \approx 10^5 y$$





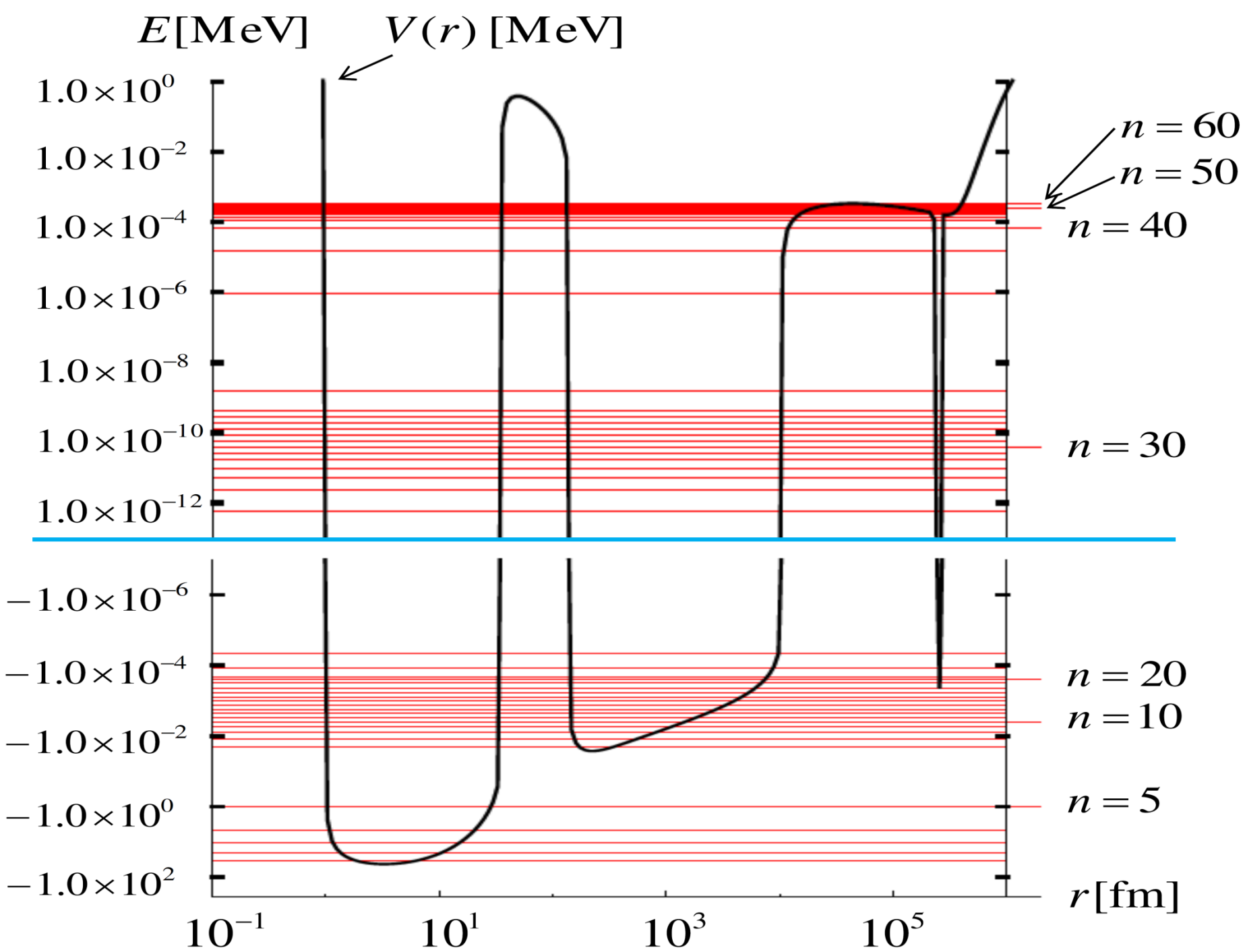
GPT-potential is given by parameters  $a$  and  $\gamma$  and

a potential depth  $V_0 (< 0)$ .

$$V^{GPT}(r) = V_0 \frac{a^{2\gamma+2}}{r(r/2+a)^{2\gamma+2}}$$

$\gamma$	$r \ll a$	GPT-potential	$a \ll r$
-1	$V_0/r$	$V_0/r$	$V_0/r$
-1/2	$V_0 e^{-r/2a} / r$	$V_0(2a) / [r(r+2a)]$	$V_0(2a) / r^2$
0	$V_0 e^{-2r/2a} / r$	$V_0(2a)^2 / [r(r+2a)^2]$	$V_0(2a)^2 / r^3$
1/2	$V_0 e^{-3r/2a} / r$	$V_0(2a)^3 / [r(r+2a)^3]$	$V_0(2a)^3 / r^4$
1	$V_0 e^{-4r/2a} / r$	$V_0(2a)^4 / [r(r+2a)^4]$	$V_0(2a)^4 / r^5$
3/2	$V_0 e^{-5r/2a} / r$	$V_0(2a)^5 / [r(r+2a)^5]$	$V_0(2a)^5 / r^6$
2	$V_0 e^{-6r/2a} / r$	$V_0(2a)^6 / [r(r+2a)^6]$	$V_0(2a)^6 / r^7$
...			





# 第1章

Efimov effect (エフィモフ効果)と  
長距離ハドロンポテンシャルの予言

# Review of Efimov-effect

**Efimov V.** Energy levels arising from resonant two-body forces in a three-body system, Phys. Lett. **B33**, 563 (1970)

**Efimov V.** Energy levels of three resonantly interacting particles, Nucl. Phys. **A210** 157 (1973)



- 1) the **scattering length** of the sub-system should be  $a \rightarrow \infty$  (**the first criterion**)
- 2) three-body **binding energies condense** on the three-body **break-up threshold (3BT)** where the energy level structure is given by
$$E_n / E_{n+1} = \text{constant} > 1 \quad (n: \text{quantum number})$$
(**the second criterion**)
- 3) energy level **can be obtained by**  
 $r^{-2}$  potential (**the third criterion**)

**Nicholson A.F.**, Bound states and scattering in an  $r^{-2}$  potential  
Australian J. Phys **15**, 174-179 (1962)

# Review of Efimov-effect

**Efimov V.** Energy levels arising from resonant two-body forces in a three-body system, *Phys. Lett.* **B33**, 563 (1970)

**Efimov V.** Energy levels of three resonantly interacting particles, *Nucl. Phys.* **A210** 157 (1973)

**Kraemer T. et al.**, Evidence for Efimov quantum states in an ultracold gas of caesium atoms. *Nature* vol. **440**, pages **315–318** (**2006**)

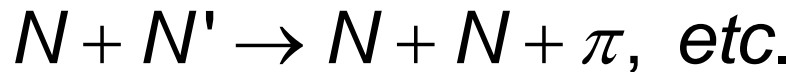
In the **hadron systems**:

- 1) The **first criterion** :  $a_{NN} \neq \infty$ ,  $a_{N\pi} \neq \infty$   
ほぼ考えられない！
- 2) The **second criterion** is that there are some instances that **energy levels come near the threshold** region. However, it is **very hard to confirm** whether they are Efimov levels or not.  
エネルギー0近傍では実験的検証が困難！
- 3) The **third criterion** is that the **nuclear potential** is usually **a short-range**: **one pion exchange Yukawa** potential etc.  
湯川ポテンシャルは短距離力である！  
 $1/r^2$  のようなポテンシャルは考えられない。

# I. General particle transfer (GPT)-potential

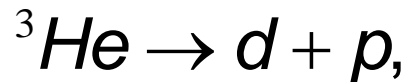
We reevaluate the Efimov physics  
by the thresholds.

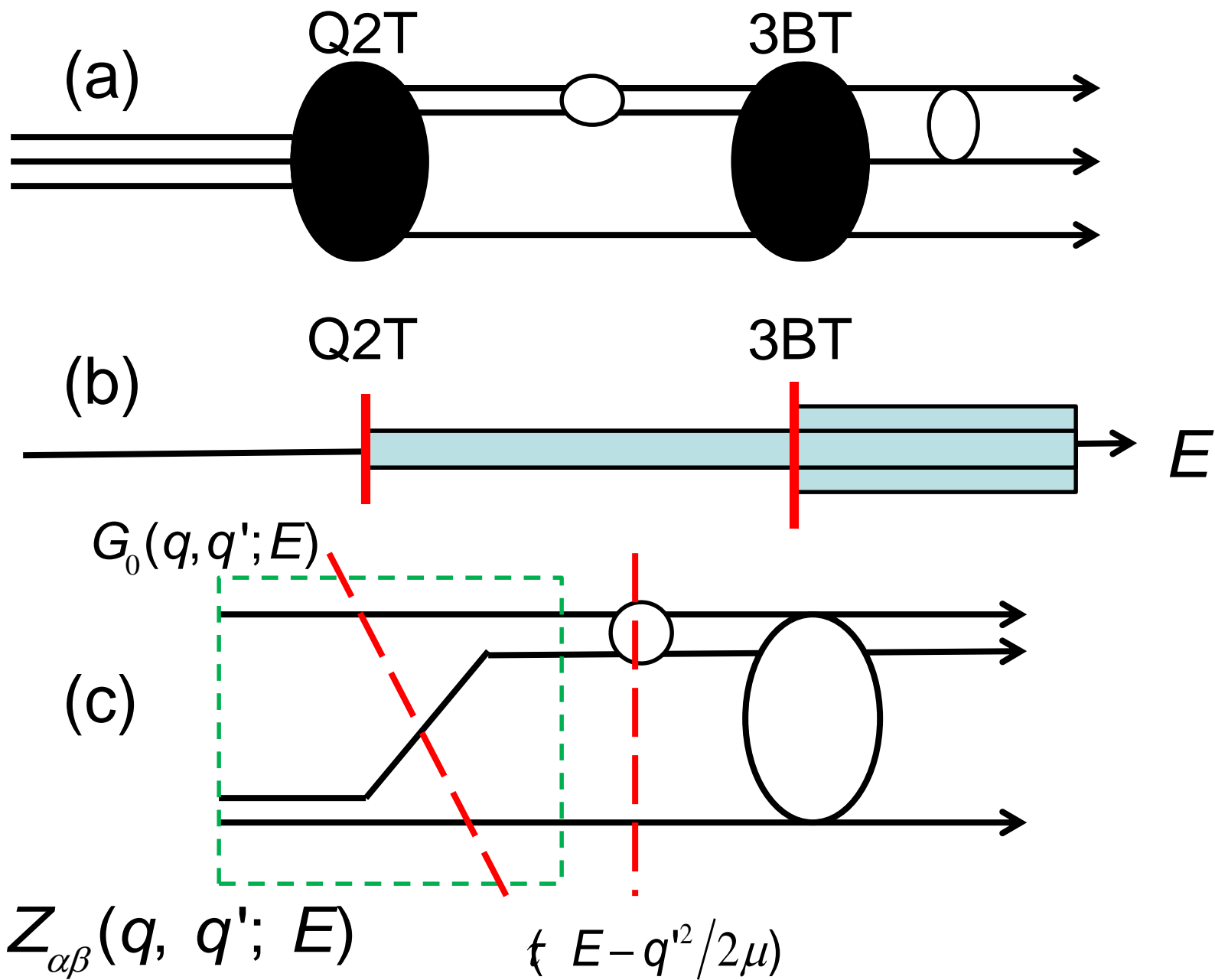
- 1) Pay attention to the three-body break-up thresholds (3BT) : appear in reactions:



- 2) From 3-body bound state to the quasi two-body system:

quasi two-body threshold (Q2T) :

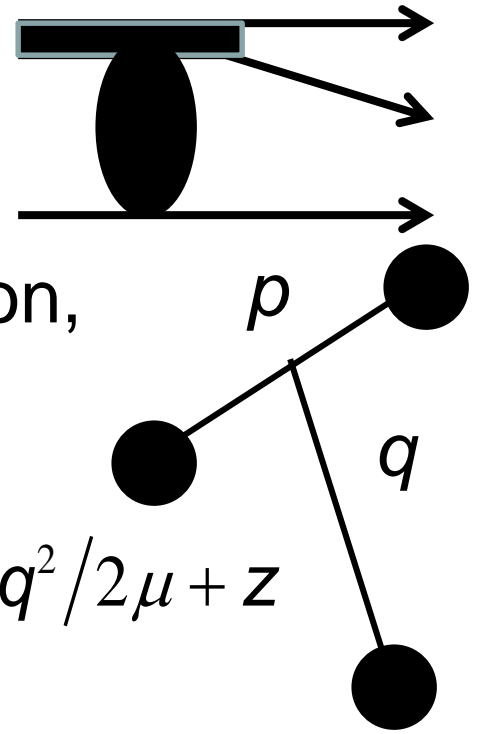






# 1) At the 3BT,

the **Born term Z** of the Faddeev or the Alt-Grassberger-Sandhas (AGS) equation, and the **propagator** have singularities;



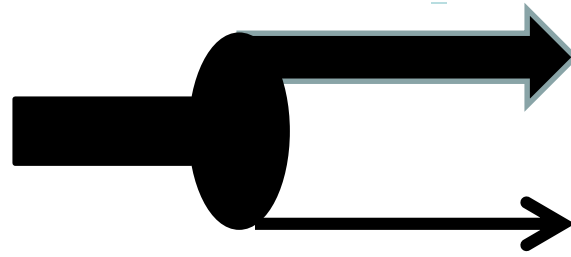
At 3BT ( $E = 0, q = p = 0$ ) : by using  $E = q^2/2\mu + z$

$$Z_{\alpha\beta}(q, q'; E) = \frac{g_{\alpha}(p)g_{\beta}(p')(1 - \delta_{\alpha\beta})}{E - q^2/2\mu - p^2/2\nu} \rightarrow \infty$$

$$\langle z \rangle = \langle E - q^2/2\mu \rangle = \frac{f(z)}{\varepsilon_B + z} \Rightarrow \frac{f(z)}{z} = \frac{f(z)}{E - q^2/2\mu} \rightarrow \infty.$$

$$\text{or } \langle z \rangle \propto \frac{1}{-1/a - ik} \rightarrow \lim_{a \rightarrow \pm\infty} i \frac{\sqrt{2\nu}}{\sqrt{E - q^2/2\mu}} \rightarrow i\infty.$$

2 ) At the Q2T:



a) Propagator: at Q2T, with  $E = q^2 / 2\mu + z$

$$\tau_B(z) = \frac{f(z)}{\varepsilon_B + z} = \frac{f(z)}{(\varepsilon_B + E) - q^2 / 2\mu} \rightarrow \infty$$

for  $E_{cm} = E + \varepsilon_B = 0, q = 0$

Apart from AGS, an Energy dependent Two-body Quasi( E2Q) potential with two-body bound state ( or  $a \neq \infty$ ) becomes by using on-shell condition for Q2T.





# Numerical calculation for GPT- Efimov-like potential

$n$	$E_n$	$E_n/E_{n+1}$	$\langle r_n^2 \rangle^{1/2}$	$\langle r_n^2 \rangle^{1/2} / \langle r_{n+1}^2 \rangle^{1/2}$
1	-2.222		2.516	
2	$-1.271 \times 10^{-2}$	174.8	$3.652 \times 10^1$	14.52
3	$-7.433 \times 10^{-5}$	171.0	$4.812 \times 10^2$	13.18
4	$-4.347 \times 10^{-7}$	171.0	$6.296 \times 10^3$	13.08
5	$-2.543 \times 10^{-9}$	171.0	$8.233 \times 10^4$	13.08
6	$-1.487 \times 10^{-11}$	171.0	$1.077 \times 10^6$	13.08
7	$-8.697 \times 10^{-14}$	171.0	$1.408 \times 10^7$	13.08
8	$-5.087 \times 10^{-16}$	171.0	$1.841 \times 10^8$	13.08
9	$-2.975 \times 10^{-18}$	171.0	$2.407 \times 10^9$	13.08
10	$-1.740 \times 10^{-20}$	171.0	$3.147 \times 10^{10}$	13.08

Our analytic prediction fits to the numerical solution.

